Equilibrium partitioning of naphthenic acid mixture part 1: Commercial naphthenic acid mixture

Are Bertheussen*, Sébastien Simon and Johan Sjöblom

Ugelstad Laboratory, Department of Chemical Engineering, the Norwegian University of Science and Technology (NTNU), N-7491 Trondheim, Norway
are.bertheussen@ntnu.no, sebastien.c.simon@ntnu.no, johan.sjoblom@ntnu.no

Abstract:
Crude oil contains naphthenic acids that can partition into water. This phenomenon is a function of several parameters like the naphthenic acid composition, pH and water phase salinity. This article is a continuation of previous work regarding the partitioning between oil and water of model acids and bases in model systems with regards to pH and salinity. The present work will focus on a commercial naphthenic acid mixture from Fluka while the next work will deal with extracted naphthenic acids from a crude oil. The composition of the acid mixture was determined by GC/MS and it was found that the commercial naphthenic acid mixture is mostly composed of saturated acids with 0 to 3 ring structures. The partitioning of the commercial naphthenic acid mixture was determined. The equilibrium partitioning of acids with different molecular weight was determined over a large pH interval using toluene as the oil phase and 3.5wt.% NaCl aqueous buffers as the water phase. The partitioning of the naphthenic acid mixture with pH was successfully modelled by dividing the naphthenic acid mixture into narrow molecular weight range fractions characterized by a single partitioning ratio, pP_{wo}. The variation of the pP_{wo} of the fractions with molecular weight was found to be linear. In presence of calcium and high pH the partitioning of higher molecular weight acids was reduced, likely due to formation of oil soluble calcium naphthenates since no precipitation was observed. The partitioning of low molecular weight acids was not affected by calcium.

*To whom correspondence should be addressed.

Telephone: (+43) 73 55 09 24.
E-mail: are.bertheussen@ntnu.no

Keywords
Equilibrium partitioning
GC/MS
Naphthenic acids
Partition ratio

1. Introduction

As the world energy demand continues to increase, energy companies prepare to utilize more complicated oil resources [1, 2]. Biodegraded crude oil can be more difficult to produce due to its lower API gravity, elevated total acid number (TAN) and total base number (TBN) [3-5]. These acids and bases in crude oil can partition and solubilize into the co-produced water phase, a tendency that is affected by parameters like pH, temperature and molecular weight.

Subsea solutions for produced water discharge and achieving export quality crude oils subsea are close to becoming a reality [6]. To predict how the oil and water quality will be affected by inlet conditions like the composition and properties of the well stream over the fields lifetime, more knowledge is needed about the partitioning behavior of crude oil components like naphthenic acids. This paper is the first in a series of 2 to discuss and explore the composition and equilibrium partitioning of naphthenic acid mixtures.

2. Theory

2.1. Definition and prevalence

The term “naphthenic acids” has been used to describe all organic acids found in crude oil although the traditional definition describes a carboxylic acid with a naphthene ring. The weight percent in crude oil varies from 0 wt.% to 3 wt.% [7]. As

with other crude oil components, naphthenic acids have large variations in size and structural conformations, however a good rule of thumb is that they have a molecular weight between 200-700 g/mol [8] and a structure described by the isomer $C_nH_{2n+Z}O_2$ [9]. So-called oxy-naphthenic acids $C_nH_{2n+Z}O_x$ isomer formulas have also been used to include naphthenic acids with added hydroxyl or acidic functional groups [10]. In either case the *n* refers to the number of carbon atoms, while the *Z* is a negative integer referring to the hydrogen deficiency of the naphthenic acid molecule, the *x* refers to the number of oxygen atoms. This view of naphthenic acids however, might be too limiting as noted by Grewer, Young, Whittal and Fedorak [10] who reported that less than half of the peak abundancies in the acid oil extracts and commercial examined could be grouped into the $C_nH_{2n+Z}O_x$ isomer. Headley, et al. [11] defined the term naphthenic acid fraction components (NAFC) which allowed for more combinations with functional groups containing oxygen, sulphur, nitrogen and aromatic rings. Qian, et al. [12] in their identification of 3000 acids from a south American crude oil found that crude oil acids range from C_{15}-$C_{55.}$ Several authors [12-14], have concluded, after experimenting with crude oils from North, Central and South America, that less than half the acids are "true naphthenic acids", while the rest consists of acids with one or more aromatic, nitrogen or sulphur groups like alkyl sulphonic acid. Hemmingsen, et al. [15] on the other hand, found acids from a North Sea crude oil to consists predominantly of conventional naphthenic acids i.e. molecules with one carboxyl group.

Naphthenic acids are corrosive [16] although using TAN as an indicator for corrosiveness is unreliable and researchers suspect a smaller subgroup of acids might be culpable [13]. Naphthenic acids affect the stability of water in oil emulsions and oil in water emulsions [17, 18] and cause pipe or formation pore blockage through precipitation [19, 20]. Some of the cyclic and aromatic naphthenic acids has been shown toxic and carcinogenic [21] which is why dissolved naphthenic acids are considered major contaminants in oil sands process-affected water (OSPW) [22]. Produced water discharge from offshore installations also contains naphthenic acids which raises some environmental concerns [23].

Mass spectrometry has been extensively used to characterize naphthenic acids in multiple studies [10, 12-14, 24-31]. With high resolution MS, such as FT-ICR MS, the abundance of each isomer can be extracted from the mass spectra to obtain the composition of the naphthenic acids in the sample [32]. However, this technique presents some pitfalls. For instance, Clingenpeel, et al. [33] performed FT-ICR MS on

fractions according to their hydrophobicity from acidic interfacial material isolated from a bitumen sample. They revealed that when analyzed unfractionated, the most ionizable compounds i.e. the least hydrophobic, low molecular weight monoacids masked the presence of larger compounds. Fractionation showed that the acid fraction that gave the tightest emulsion was composed of asphaltene-like acids with regards to size and aromaticity. Stanford, et al. [34] used FT-ICR MS to compare the composition of the polar components of nine crude oils to the surface-active material from the corresponding crude oil. They found that in general the DBE and carbon number distributions of the interfacial material overlaps with the polar components of the parent crude oil. For water soluble species however, the distributions of polar species do not match that of the parent oil. Less hydrophobic species like acids with aromatic ring structures would for example be relatively more abundant in the water phase [28].

Jones, et al. [35] developed a GC/MS method for routine quantification of naphthenic acids in both light and heavy oils. Scott, Young and Fedorak [25] also describes a quantitative naphthenic acid detection method based on GC/MS [36, 37] which exploits the general absence of C_{13} acids in nature. When used in comparison with results obtained from FTIR, they found that in all but one case, the FTIR results showed higher concentrations than the GC/MS, often 2-4 times higher. This difference was attributed to hydroxy-naphthenic acids not being included in the GC/MS quantification. St. John et al. (1998) developed a GC/MS method which uses N-methyl-N-(t-butyldimethylsilyl) trifluoroacetamide (MTBSTFA) to derivatize naphthenic acids to their t-butyldimethylsilyl esters. This derivatization method produces a stable ion fragment [M+57] where M is the molecular weight of the naphthenic acid. Through these characteristic ions, individual components eluting within the usually large, unresolved hump of naphthenic acids can be classified, providing the composition of the naphthenic acids based on *Z* and carbon numbers [26]. This method has later been applied by several authors [25, 26, 36, 38-40]. On testing multiple derivatization agents on different model acid structures Shepherd, van Mispelaar, Nowlin, Genuit and Grutters [40] found MTBSTFA to give one of the best yields overall although recent research claim pentafluorobenzyl bromide (PFBBr) to be superior to MTBSTFA [41].

Mass spectrums of commercially available NA mixtures and OSPW or crude oil extracts have been studied by several authors [8, 10, 13, 14, 36, 42-48] and Saab, et al. [49] discusses various naphthenic acid extraction methods. In general researches found

commercial acid mixtures to contain more saturated and lighter acids compared to acids extracted from crude oil or oil sand. Caution should be used when comparing obtained results with previously published data as West, et al. [50] warns that different batches of commercially available NA mixtures from the same vendor might differ.

2.2. Oil-water partitioning

Some crude oil components have some solubility in water. Hydrophobic surface area is inversely related to the aqueous solubility [51]. Alkyl chains increase hydrophobic surface area whilst branching, polar or aromatic groups decrease this area [28]. Production alterations in pH, pressure, temperature also affect solubility [52], in effect changing the composition of the oil and water phase. The polarity of the crude oil acids makes them more water soluble than their non-polar counterparts. The partitioning of naphthenic acids between oil and water strongly depends on the pH of the aqueous phase. At low pH, naphthenic acids are neutral and their solubility in water is limited. As the pH increases naphthenic acids are ionized and, therefore, their partitioning in the aqueous phase increases. The ionization of acids is classically characterized by an acid constant, pK_a. The pK_a of short chain acids is close to 5. However, higher values have been reported for long chain acids[53]. Kanicky and Shah [53] have shown that pK_a decreases with the concentration of acid and reaches values close to 5 at infinite dilution. This behavior was attributed to the presence of long chain acid premicellar aggregates, which at higher concentrations would influence acid-base equilibria. Upon extracting crude oil acids with neutral water, Stanford, Kim, Klein, Smith, Rodgers and Marshall [28] detected water soluble acids up to C_{41}(~600 g/mol). The extent of the partitioning depends on the structure (hydrophobicity) of the naphthenic acid. In his study of naphthenic acid partitioning Havre, Sjöblom and Vindstad [42] found that naphthenic acids in crude oil water systems had a pK_a of 4.9, which corresponds to the pK_a range reported by Brient, et al. [54], and varying pP_{wo} depending on the molecular weight of the acids. Different partitioning models are reported in literature. The most comprehensive one found was covered in Touhami, et al. [55] which includes most of the equilibria encountered in oil water systems, i.e. partitioning of indigenous polar compounds and added surfactants, dissociation, micellization and even metal naphthenate partitioning back into the oil phase. Based on previous models [42, 56], Hutin, et al. [57] developed a model

that could predict the final pH of a crude oil water system based on the TAN, TBN and initial pH.

In this study, the equilibrium partitioning of a commercial NA(naphthenic acids) mixture will be considered over the pH range. The goal is to determine the partition ratio for acids and obtain insight into how molecular weight influences the behavior of these compounds in two phase systems.

2.3. Modelling of partition ratio with pH

In this section a classical thermodynamic model for the partitioning of naphthenic acids is presented. This model has for instance already been applied by Havre, Sjöblom and Vindstad [42,] Nordgård, et al. [58,] Bertheussen, et al. [59] and others in their work.

In an oil-water system, the acids in their protonated form would partition themselves between the phases according to the following partition constant

$$K_{wo,HA} = \frac{[HA]_w}{[HA]_o} \qquad (1)$$

where $[HA]_w$ represents the protonated acid concentration in the water phase, $[HA]_o$ represents the acid concentration in the oil phase and $K_{wo,HA}$ represents the partition constant of the acid. This partition constant is independent of concentration, but varies with temperature and pressure. Due to dimer considerations discussed in a previous article [59] the partition ratio defined by Scherrer and Howard [60] will be used in the following models. The ratio accounts for the non-ionized compounds in each phase as seen in Equation 2.

$$P_{wo} = \frac{[HA]_w}{[HA]_{o,tot}} = \frac{[HA]_w}{[HA]_o + 2[(HA)_2]_o} \qquad (2)$$

In the water phase, the acids can also deprotonate/protonate as described by the following dissociation constant

$$K_{a,HA} = \frac{[A^-]_w[H^+]}{[HA]_w} \qquad (3)$$

where $[A^-]_w$ represents the concentration of dissociated acid in the water phase and $K_{a,HA}$ represents the dissociation constant of the acid. By introducing some new terms, the following mass balance can be applied to the system,

$$[HA]_{o,init}\,V_o = [HA]_{w,tot}V_w + [HA]_{o,tot}V_o \qquad (4)$$

where $[HA]_{o,init}$ represents the initial concentration of acid in the oil phase, and $[HA]_{w,tot}$ represents the sum of dissociated and undissociated acids in the water phase. The terms V_o and V_w denote the volume of the oil and water phase.

The equation sets consisting of Equations (2, 3, 4) can be combined to form an expression for the total acid content in the water phase and oil phase as presented below.

$$[HA]_{w,tot} = \frac{[HA]_{o,init}}{\frac{[H^+]}{P_{wo,acid}(K_{a,HA}+[H^+])}+\frac{V_w}{V_o}} \qquad (5)$$

$$[HA]_{o,tot} = \frac{[HA]_{o,init}}{1+\frac{V_w P_{wo,acid}(K_{a,HA}+[H^+])}{V_o[H^+]}} \qquad (6)$$

It is assumed that the deprotonated acid [A^-] is completely insoluble in oil phase. With divalent cations in the oil phase other phenomena like the formation of oil soluble naphthenates [61] and precipitation of metal naphthenates [62] can occur. Since the production problems with calcium naphthenates were first encountered in the 1990's [19], there has been much research on the effect of divalent cations on naphthenic acids in oil water systems [7, 8, 63-66] and therefore part of this article is dedicated to this effort.

This article aims to assess how a petroleum cut commercial acid mixture partitions between the oil phase and the water phase. After characterization of the naphthenic acid and molecular weight mostly by GC/MS, the influence of molecular weight on oil-water partitioning will be determined. The partition ratio P_{wo} will be obtained through fitting Equations 5 and 6 with a constant pK_a of 5. The effect of divalent cations on the partitioning behavior of the acids will be evaluated to determine if Ca^{2+} has specific interaction with the naphthenic acid mixture. This study will be extended for naphthenic acid mixtures extracted from crude oil in a part II article. Data obtained through these studies will be used as a basis for ongoing studies into the kinetics of acid partitioning. An acid mixture from Fluka was chosen as the commercial acid mixture in this study because it contains both aliphatic and alicyclic acids as previously shown in Lo, Brownlee and Bunce [46,] Hindle, Noestheden, Peru and Headley [47]

3. Materials and methods

3.1. Chemicals

The following chemicals was used as received from the manufacturer without further purification: Toluene (Sigma Aldrich Anhydrous 99.8%), deuterated chloroform (Sigma Aldrich, 99.96atom% D), n-tert-Butyldimethylsilyl-N-methyltrifluoroacetamide with 1% tert-Butyldimethylchlorosilane (MTBSTFA + 1% TBDMSCl) (Sigma Aldrich ≥95%), acetic acid (Sigma Aldrich, >99.99%), potassium dihydrogen phosphate (Merck, ≥ 99.5%), sodium tetraborate decahydrate (Sigma Aldrich, ≥ 99.5%), sodium chloride (Merck, 99.5%), sodium bicarbonate (Sigma Aldrich, 99.5%), calcium chloride dihydrate (Sigma Aldrich, 99%). A commercial naphthenic acid mixture from Fluka was used with specifications from manufacturer; density (d_4^{20}) 0.95, acid number 230 mg_{KOH}/g and it looks like a thick golden liquid. Different carboxylic acids were used to test the GC/MS procedure, their features are listed in Table 1.

Table 1. List of chemicals used as model acids, their molecular weight, supplier, purity, stable mass fragment after derivatization with MTBSTFA referred to as [M+57] where M is the molecular weight of the acid, the actual mass difference between the molecular weight of the acid and the stable ion fragment, the abundances of the stable ion fragments, mass of the isotope +2, abundance of the isotope +2. All abundances are calculated based on the sum of fragment intensities which match naphthenic acid masses (cut off 159 m/z) listed in Table S1.

Acid (C number, Z number)	Molecular weight [g/mol]	Supplier	Purity %	Stable ion fragment after derivatization [M+57]*** [m/z]	Mass difference [m/z]	[M+57] abundance %	[M+57]+2 isotope [m/z]	[M+57]+2 isotope abundance %
3-Cyclopentylpropionic acid (8,-2)	142	Aldrich	98%	199	+57	92 %	201	5 %
Propyl benzoic acid (10,-8)	164	Aldrich	97%	221	+57	95 %	223	0 %**
Cyclohexanebutyric acid (10, -2)	170	Acros organics	99%	227	+57	89 %	229	5 %
Capric acid (10, 0)	172	Fluka	99%	229	+57	96 %	231	0 %**
5-phenylvalerian acid (11,-8)	178	Aldrich	99%	235	+57	97 %	237	0 %**
1-Naphthaleneacetic acid (12, -14)*	186	Sigma	>95%	243	+57	92 %	245	0 %**
trans-4-Pentylcyclohexanecarboxylic acid (12, -2)	192	Acros organics	98%	255	+57	91 %	257	5 %
Tridecanoic acid (13, 0)	214	Fluka	99,7%	271	+57	89 %	273	6 %
4-heptylbenzoic acid (14, -8)	220	Alfa Aesar	99%	277	+57	76 %	279	5 %
Myristic acid (14, 0)	228	Acros organics	99.5%	285	+57	89 %	287	6 %
Palmitic acid (16, 0)	256	Sigma Aldrich	99%	313	+57	87 %	315	6 %
6-heptylnaphthalene-2-carboxylic acid (18,-14)*†	270	Chiron AS	99.9%	327	+57	61 %	329	5 %
Stearic acid (18, 0)	284	Fluka	97%	341	+57	85 %	343	6 %
Hexadecanedioic acid (16, 0)*	286	Fluka	98%	457	+114+57	61 %	459	8 %
Behenic acid (22,0)	341	Fluka	99%	398	+57	80 %	399	7 %
5β-Cholanic acid (24, -8)	360	Sigma	99%	417	+57	44 %	419	4 %
Docosanedioic acid (22, -0)*	370	Sigma Aldrich	95%	541	+114+57	52 %	543	9 %

Indicates a structure which does not match how this ion would be attributed on the mass distribution Table S1 which assumed only monoacids and Z ≤ 12. 1-Naphthaleneacetic acid (12, -14) would for instance be counted as a C=11, Z=0 acid while Docosanedioic acid would be counted as a C=33, Z=-10 acid. **Indicates that this value would not be counted as it does not fit into the naphthenic acid mass distribution table (Table S1) given in the supporting information.*For simplicity [M+57] is also used to describe stable ion fragment for diacids, even though it technically should be [M+57+114]. † Internal standard. Acid abundances do not add up to 100% due to the presence of other ion fragments. The isotope +1 is not included in calculations for this table as it does not fit into the naphthenic acid mass distribution table (Table S1) given in the supporting information*

3.2. Characterization

Hydrogen 1 (^{1}H) and Carbon 13 (^{13}C) nuclear magnetic resonance (NMR) were obtained with a Bruker Avance NMR spectrometer (400 MHz). Naphthenic acid samples were prepared to a concentration of 1wt.% for ^{1}H and 10wt.% for ^{13}C in $CDCl_3$. The elemental composition (C, H, N, O, S, Ca, Cl, Na) was determined by the Laboratory SGS Multilab (Evry, France) by thermal conductivity measurements for C, H, and N, by infrared measurements for O and S, by mineralization and ICP/AES for Ca and Na and potentiometric titration for Cl. The TAN values were

determined according to the D664-95 ASTM method on a Titrando unit (Metrohm) fitted with a 6.0229.100 LL solvotrode.

3.3. Equilibrium partitioning

3.3.1. With monovalent cations

At least two parallels of oil water experiments from pH 2-12 were performed. Solutions of the commercial acid mixture in toluene were prepared at 2 different concentrations: 10 mM (2.3 g/L) and 4 mM (0.9 g/L). These concentrations correspond to TAN's between 0.25 and 0.7 mg_{KOH}/g. 3.5wt.% NaCl aqueous buffers listed in Table 2 were prepared with ultra-pure water (MilliQ resistivity of 18.2 MΩ.cm millipore) as the water phase. Equal volumes of oil and water phase (8 mL) were shaken at 250 rpm for 24 h on a horizontal shaker (IKA® HS 501). Samples were then centrifuged at 11000 rpm for 30 min. The pH was measured before contact with the oil phase and after centrifugation. The oil phase is directly analyzed as explained in section 3.4.1. while the naphthenic acids in the water phase are first extracted through the following procedure. 6 mL of the water phase was recovered and adjusted to pH<2 by adding between 0.6 to 3 mL of 1 M HCl in 3.5wt% NaCl solution depending on the pH of the aqueous buffer. Naphthenic acids present in the low pH water phase were back-extracted into a toluene volume equal to the recovered water before pH adjustment (6 mL) by shaking for 24 hours. The extraction yield was assumed 100% considering the pP_{wo} and mass balances obtained in this work. To obtain a signal for the water phase in pH 2 experiments, 200 mL of both phases were used and the oil from the back-extracted water phase concentrated through evaporation prior to analysis. After centrifugation the water phase of the experiments with the pH 11 and 12 buffers had a slightly opaque water phase.

3.3.2. With divalent cations

At least two parallels of oil water experiments were performed at pH: 7, 8.4, 9, 10, 12. The conditions were like the ones mentioned in the paragraph above except here the aqueous buffers contained 3.5wt.% NaCl and 10 mM $CaCl_2$. Another exception

was that the results for pH 7 were obtained through using a high initial pH (10.6) unbuffered solution due to $KH_2PO_4/CaCl_2$ incompatibility. Washing oil phase with low pH water was considered since calcium naphthenates would presumably be unavailable for derivatization, but this treatment was found to only affect the pH 12 sample with regards to the internal standard peak. The post-centrifugation opaqueness of the high pH buffers mentioned in the previous paragraph was not observed in these experiments.

To obtain enough dry sample for elemental analysis after equilibrium partitioning with calcium, higher volumes (450 mL of both phases) were used.

Table 2 List of different aqueous buffers prepared [67]

pH	Buffers
2	0.01 M HCl
4	0.1 M CH_3COOH adjusted with NaOH
6-7.9	0.1 M KH_2PO_4 adjusted with NaOH
8.4-9	0.025 M Borax adjusted with HCl
9.5-10	0.025 M Borax adjusted with NaOH
11	0.05 M $NaHCO_3$ adjusted with NaOH
12	0.01 M NaOH

3.4. GC/MS,

3.4.1. Preparation and analysis of the samples

0.7 g of 0.22 mM 6-heptylnaphthalene-2-carboxylic acid in toluene (used as internal standard) was added to 1.6 g of sample prior to derivatization. The criterium for the internal standard was an acid with elution time close to the hump of the acid mixture. 6-heptylnaphthalene-2-carboxylic acid was selected to elute after the commercial acid mixture. 0.36 g toluene solutions with naphthenic acids and internal standard were added to a micro-insert inside a 1.5 mL glass vial along with 0.04 g of N-tert-Butyldimethylsilyl-N-methyltrifluoroacetamide with 1% tert-Butyldimethylchlorosilane (MTBSTFA + 1% TBDMSCl) giving a >30 times excess of derivatization agent. The glass vials were sealed with Teflon lined caps and the samples were heated in a water bath at 65°C for 30 min and weighed before and after. The weight did not change. GC/MS analysis was performed on an Agilent GC(7890)/MS(5977) equipped with an Agilent J&W DB-1HT Non-polar, 100%

Dimethylpolysiloxane, capillary column (30m×0.25mm×0.10 µm film thickness). The injection was run in split less mode. The helium carrier gas flowrate was kept at 1 mL min^{-1}. The inlet temperature and the GC/MS interface temperature were both kept at 330°C. An initial temperature of 100 °C was held for 5 minutes before a ramp of 5 °C/min until a maximum temperature of 325 °C, which was held for 10 minutes. Solvent delay was set to 5 minutes. The GC/MS was operated in electron impact ionization mode with ion source temperature and quadrupole temperature at 230°C and 150°C respectively. This instrument was set to scan from m/z 42–600 with a scan rate of 5 scans/sec. An injection volume of 0.3 µL was chosen to ensure that saturation would not occur i.e. no m/z peak could exceed 8.5 x 10^6 counts. Every 5 samples, pure solvent was run with the same method to serve as a blank. Chromatograms and spectra were acquired and analyzed using the Qualitative Analysis (Masshunter Acquisition Data) program.

3.4.2. Mass chromatogram analysis

Mass spectra were extracted from the chromatogram peaks with a height filter only considering peaks with a relative height > 0.1% of largest peak. Spectra from corresponding blank solvent runs were subtracted from the sample spectra. The m/z values obtained were used to determine the NA molecular weight, the carbon number and the hydrogen deficiency (*Z*). The procedure was the following: First the m/z values were rounded by setting the values between (x-1).7 and (x).7 to x since most atoms weight more than nominal mass. For example, both 237.7 m/z and 238.69 m/z would be rounded to 238 m/z. Then the *n* and *Z* were determined using the matrix presented in Table S1 of the supporting information. This table S1 is an example of a matrix of the possible naphthenic acids within the carbon number range of 5–37, with 0–6 rings (*Z* =0 to −12), the masses shown are those of [M+ 57] ions. Some isomer combinations are excluded by on the rules set up by Holowenko, MacKinnon and Fedorak [26], for example nonexistent molecules with five carbons and 6 rings. Contrary to Holowenko, MacKinnon and Fedorak [26], aromatic structures were considered in this work. The shortcoming of MTBSTFA regarding steric hindrance [38] was not investigated.

3.4.3. Quantification

The equilibrium concentrations of both phases were determined by GC/MS. Total ion chromatograms (TIC) are chromatograms which show the sum of all intensities for all masses registered by the detector over time. The extracted ion chromatogram (EIC) shows the sum of intensities for a specific mass or mass range registered by the detector over time. The total NA concentration and the concentration of NA of specific molecular weight ranges were determined using the following methodology: Extracted ion chromatograms (EIC) were obtained from total ion chromatograms (TIC). After subtraction of solvent blanks obtained during the same analysis session and integration of the peak, the naphthenic acid concentration was determined after normalization with internal standard peak area (6-heptylnaphthalene-2-carboxylic acid, retention time 33.7 minutes) and comparison with corresponding calibration curve.

4. Results and Discussion

4.1. Characterization

4.1.1. Characterization by TAN, elemental analysis and NMR

The total acid number of the commercial NA mixture was measured to 242 mg_{KOH}/g_{oil} through titration which indicates an average molecular weight of 231 g/mol assuming monoprotic acids, in good agreement with the data provided by the manufacturer. The elemental composition of the commercial acid mixture is listed in Table 3. The acids in the commercial acid mixture contains almost no sulphur or nitrogen. Assuming pure carboxylic acids with isomer $C_nH_{2n+Z}O_2$, the percentages of C, H, O are consistent with an average combination with $n=14$ and $Z=-2$ which indicates a molecular weight of 226 g/mol, similar to the molecular weight obtained by titration. The elemental analysis compares well to the one reported on the same commercial acid by Rudzinski, Oehlers, Zhang and Najera [14]; 74.2% C, 11.23% H, 14.5% O with negligible N and S. Consequently, the average molecular weight was also equivalent, although they did not round *n* to the nearest integer.

Table 3 Elemental composition of the commercial naphthenic acid mixture

Element	Symbol	Composition [wt.%]
Carbon	C	74.1
Hydrogen	H	11.54
Oxygen	O	14.26
Sulphur	S	<0.1
Nitrogen	N	<0.05

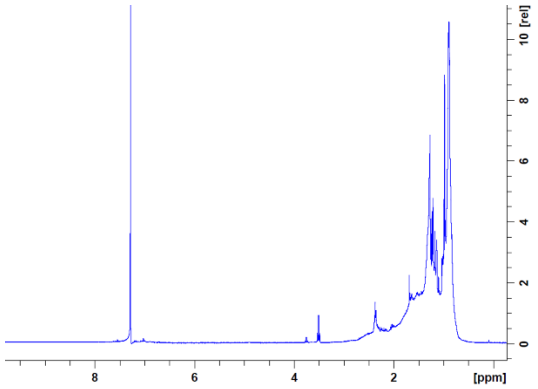

Figure 1 [1]H NMR spectrum for the commercial naphthenic acid mixture in $CDCl_3$.

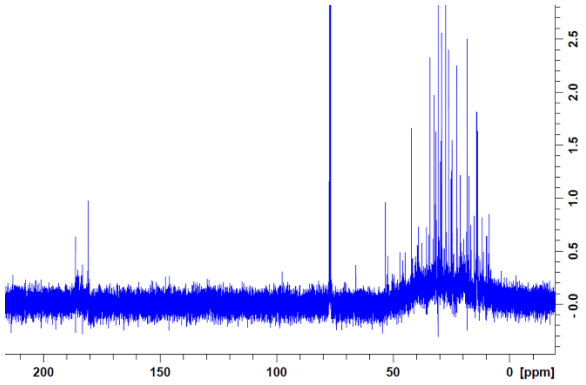

Figure 2 [13]C NMR spectrum for the commercial naphthenic acid mixture in $CDCl_3$.

^{1}H NMR and ^{13}C NMR spectra of the commercial NA mixture are depicted in Figure 1 and Figure 2. Figure 1 show the ^{1}H NMR spectrum conducted on a 1wt.% solution of the commercial acid mixture. The peaks with chemical shifts lower than 1 ppm are related to termination methyl groups, while peaks between 1.15-2.33 ppm corresponds to CH_2 methylene bridges with increasing proximity to the carboxyl group [68, 69]. The absence of peaks at 7-8 ppm indicate that there are few or no aromatic groups in the commercial naphthenic acid mixture [49]. The ^{13}C NMR spectrum performed on 10 wt.% solution shown in Figure 2 concur with these findings by showing an almost negligible intensity hump at 130 ppm for aromatic carbons. As with the hydrogen spectrum, most of the signal is in the aliphatic (primary to quaternary) region from 5-60 ppm. The peak at 180-185 corresponds to COOH, and there are no noticeable peaks from C-O bonds. Rudzinski, Oehlers, Zhang and Najera [14] in performing a ^{13}C NMR analysis on a commercial acid mixture from the same vendor reported a composition of 7.1% aromatic carbons. However as argued by West, Jones, Scarlett and Rowland [50] commercial acid mixtures from petroleum cuts might differ, even when supplied by the same vendor. This might be attributed to shifts in crude oil stock or refinery strategies.

4.1.2. Characterization by GC/MS

4.1.2.1. Assessment of derivatization efficiency

More information about the composition of acid mixtures can be determined by GC/MS. Prior to the analysis of the commercial NA mixture, the performances of the chosen derivatization agent (MTBSTFA) was investigated using model acids of known structure (Table 1). MTBSTFA derivatizes hydroxyl, carboxyl, thiol groups and primary and secondary amines and creates stable ion fragments [M+57] where M is the molecular weight of the acid [70]. To avoid confusion, mass fragments of MTBSTFA derivatized acids will always be denoted with m/z and the real molecular weights of acids will be denoted with g/mol. For simplicity [M+57] is used to describe stable ion fragment for acids with multiple functional groups like diacids as well, even though it technically should be denoted [M+57+114] for diacids (Table 1). A table of masses for the isomer $C_nH_{2n+Z}O_2$ is listed as Table S1 in the supporting information. This table allows the ascertainment of *n* and *Z* from their molecular weight as explained in section 3.4.2.

The double bond equivalent (DBE) described in Equation 7 [71] gives the average unsaturation for naphthenic acids structures. Double bond equivalents can be attributed to hydrogen deficiency *Z* as denoted in Equation 8 [72] .

$$DBE = \frac{2C+2-H}{2} \quad (7)$$

$$Z = -2DBE + 2 \quad (8)$$

where *C* and *H* are the number of carbon and hydrogen atoms in the formula. Since alkenes are typically not present in crude oil [73], hydrogen deficiency *Z* is used to assign cyclic or aromatic structures.

Acids with aromatic functional groups have traditionally been excluded from the $C_nH_{2n+Z}O_2$ isomer mass tables, either because they fall outside the traditional definition [26] or because low molecular weight aromatic acids are present in very low concentrations in petroleum acid extracts [35]. Larger aromatic acids are however present in both oil sands and petroleum [74, 75] and this article has included aromatic ring combinations as seen in Table S1, to cover as diverse a range of carboxylic acids

as possible. Indeed, *Z* can be lower or equal to -8 in Table S1 which could match molecules containing one aromatic ring.

A mixture of model acids from Table 1 was derivatized with MTBSTFA and analyzed with GC/MS. As can be seen in Figure 3 the derivatization method produces a single dominant mass fragment for different acid structures, like saturated, diacids, aromatic and polycyclic. It appears that the dominance of the single ion fragment is more evident for saturated acids and single ring acids compared to aromatic and polycyclic acids. This is also evident when evaluating the acid fragmentation findings by Clemente and Fedorak [39] who wrote a comprehensive analysis about GC/MS analysis of naphthenic acids derivatized by MTBSTFA. Their method compares how the acid fragments would be interpreted by the mass distribution matrix given in Table S1 in the supporting information (note that the isotope [M+57]+1 would not be counted in this matrix). In general, the ion abundance of the stable mass fragment [M+57] declines both with molecular weight and hydrogen deficiency. Larger acids can also give a false presence of another acid. For example, as can be seen in Table 1, around 9% of the real Behenic acid (C_{22} Z=0) peak would appear as a C_{23} Z=-12 acid due to the isotopes of carbon and silicon. However, this isotope bias in the determination of the naphthenic acid distribution is statistically insignificant as shown by Clemente and Fedorak [39].

The mass spectra of 5-phenylvalerian acid, propyl benzoic acid and 1-naphthaleneacetic acid present a higher fragmentation which is consistent with their aromaticity. However, the intensity abundance of the stable [M+57] peak indicated in Table 1 is very high (respectively 97%, 95% and 92%). This discrepancy comes from the fact that the fragments from these compounds are too small to be counted as naphthenic acids in Table S1.

The excessive fragmentation of compound with higher molecular weight, aromatic rings or polycyclic structures would create a distribution bias towards low molecular weight acids and should be considered when making mass distributions of naphthenic acids mixtures. The opposite effect where smaller acids appear to be larger acids can also occur in the situation when for example two methyl silyl groups are grafted onto a diacid. The results obtained in Table 1 show that the base peak for derivatized diacids (hexadecanedioic acid, docosanedioic acid) corresponds to [M+57+114] i.e. both acid groups have been derivatized but only one has been subsequently ionized. This was also noted by St. John, Rughani, Green and

McGinnis [24] on the diacid camphoric acid. As a result, docosanedioic acid ($C_{22}H_{42}O_4$) would appear as a monoacid with C_{33} and Z=-10 in our analysis. Similar conclusions were drawn by Bataineh, et al. [76] for hydroxylated acids. Some diacids are nevertheless doubly ionized, [M+57+57]/2 (242 m/z peak for docosanedioic acid in Figure 3 and 200 m/z peak for hexadecanedioic acid, not shown). As the doubly charged species for both diacids tested have even m/z numbers, doubly charged ion peaks do not influence the distribution as they are not counted as naphthenic acids according to Table S1. However, this is a mere coincidence, as it can easily be demonstrated that every other diacid produces an uneven doubly charged peak which would influence the naphthenic acid distribution. For instance, the diacid $C_9H_{16}O_4$ with molecular weight 188 g/mol, would give a doubly charged ion peak at 151 m/z.

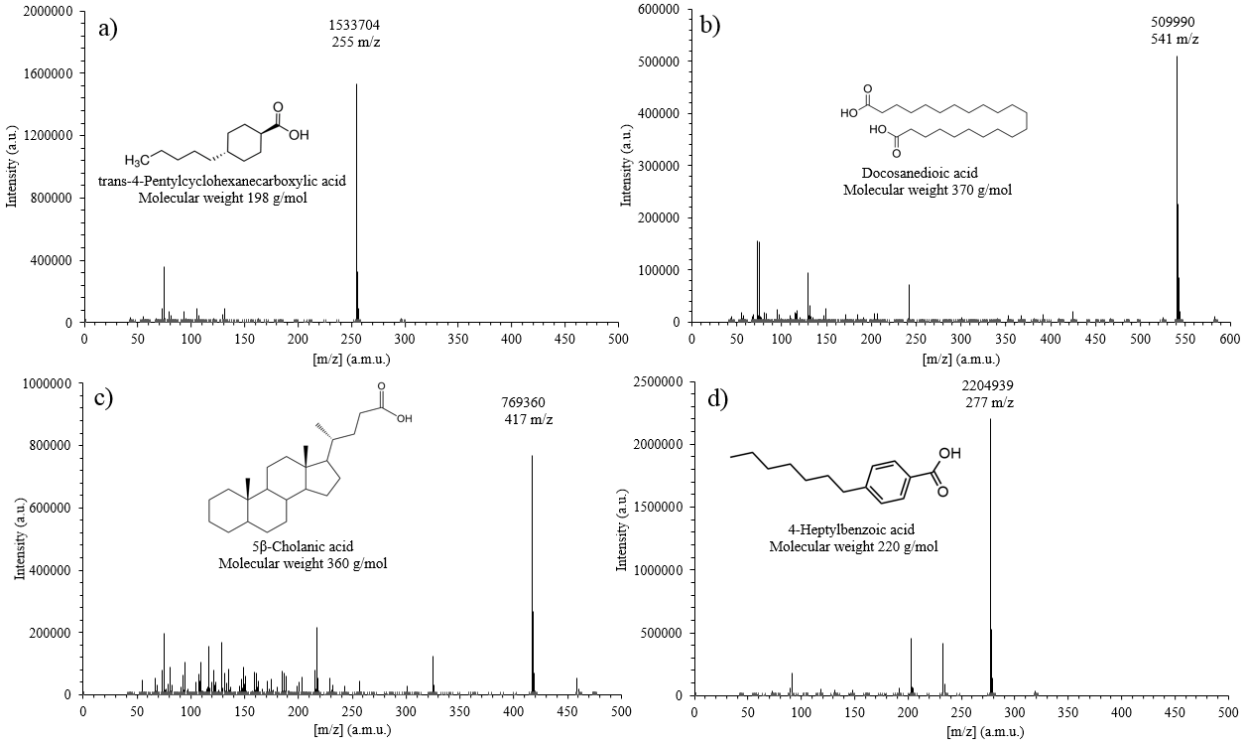

Figure 3 Mass spectrums of chromatogram peaks and structures for a) trans-4-pentylcyclohexanecarboxylic acid, b) docosanedioic acid, c) 5β cholanic acid, and d) 4-heptylbenzoic acid after derivatization with MTBSTFA.

4.1.2.2. GC/MS analysis of the commercial naphthenic acid mixture

The commercial NA mixture was analyzed by GC/MS to give the chromatogram presented in Figure 4. The chromatogram elutes as an unresolved hump with two different modes and several well-defined peaks. This means that the Fluka NA mixture is so complex that GC cannot separate all the molecules present. The well-defined peaks appear to have a hydrogen deficiency of 0 and it can therefore be speculated that they correspond to linear saturated fatty acids of different molecular weight. Their carbon numbers are indicated in Figure 4. It can be observed that saturated acid peaks elute roughly consecutively until C_{12} (retention time 19 min). at longer retention saturated C_{13}, C_{14} and C_{15} acids can be identified. As there are several peaks corresponding to C_{13} and C_{14}, it must correspond to different isomers, and consequently non-linear saturated carboxylic acids are most likely present. The second mode at retention time 25 min corresponds to molecules in C_{19}.The mass spectrum averaged over the entire elution hump was analyzed with regards to the stable mass ion fragments for naphthenic acids listed in Table S1 in the supporting information to yield a distribution shown in Figure 7. A response factor of 1 was assumed for all acids.

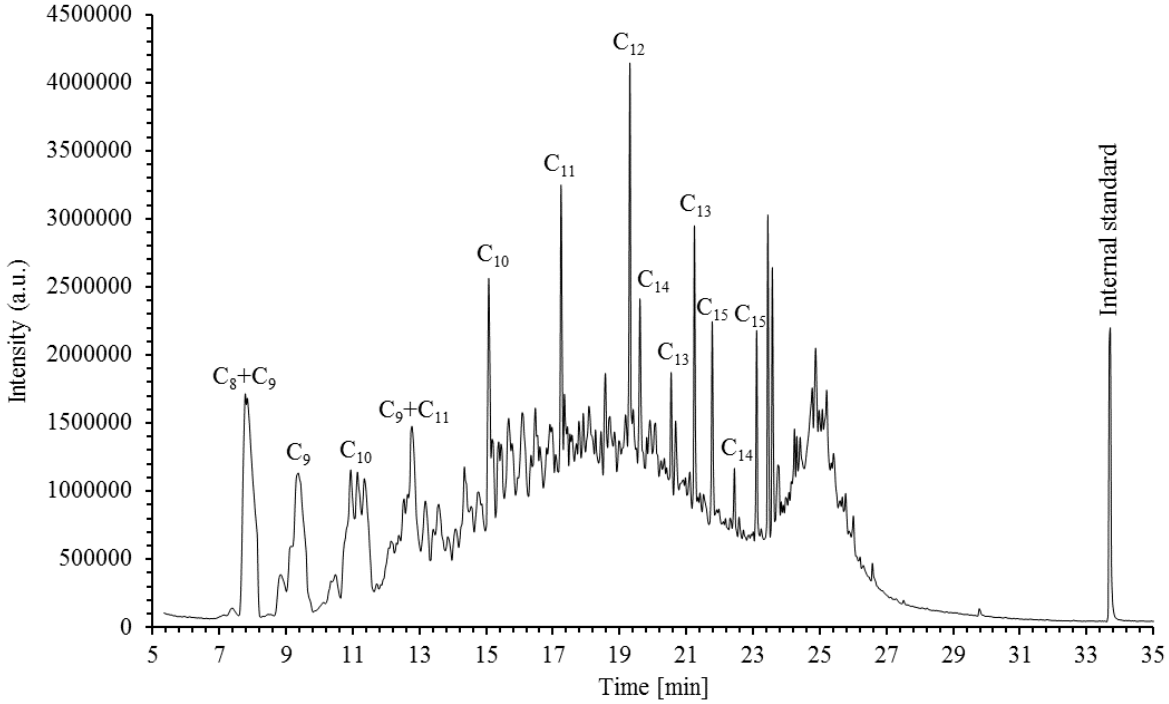

Figure 4 Chromatogram of the commercial NA mixture. The peak at retention time 33 minutes corresponds to the internal standard 6-heptylnaphthalene-2-carboxylic acid. Major peaks listed have stable ion fragments consistent with saturated fatty acids. Their carbon number is indicated on the figure.

The separation in GC fitted with nonpolar column is based on boiling point i.e. molecular weight for a given class of molecule. To check consistency of results, a visualization of increasing EIC mass ranges is shown in Figure 5. These EIC mass ranges revealed that part of the mass range 209 m/z – 233 m/z corresponding to small acids elute later in the chromatogram where acids of much larger molecular weight elute, as seen in Figure 6. These were thought to be either fragments of higher molecular weight compounds as seen in Figure 3 or non-acid pollutants. The obtained distribution also indicated a high amount (9% of the intensities corresponding to naphthenic acids in Table S1) of low molecular weight acids with stable mass fragments from 159 m/z - 208 m/z. Upon closer examination of the EIC for the mass range 159 m/z - 208 m/z, it was observed that these compounds do not elute early with a mass specific elution hump in the start of the chromatogram, but rather elute on low intensity over the entire hump. These were deemed to be fragments of high molecular weight species, hence Figure 7 starts at the next mass range 209-233 m/z or C_9. As can be seen in Table S1, the mass ranges below 209 m/z contains few possible acid structures and small molecules also have fewer structural isomers [47]. St. John, Rughani, Green and McGinnis [24] noted that it was

difficult to find masses below 200 m/z using the MTBSTFA technique on acid mixtures due to the presence of other fragment ions. The same article also argues that 97% of naphthenic acids have nine carbon atoms or more. As was seem in previous work [59], low molecular weight acids are preferably water soluble even at low pH values. Much of the reported results from the literature could be skewed in this regard as smaller acids could have been lost from the oil to the produced water or desalter water before entering the refinery.

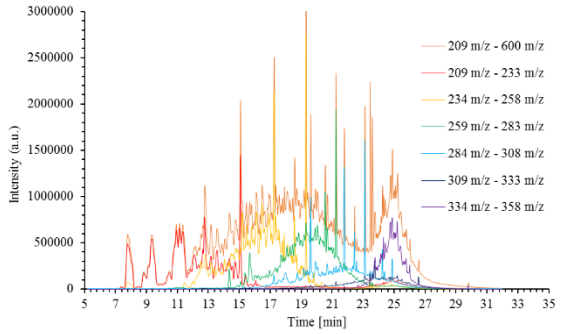

Figure 5 Chromatograms showing the EIC with mass range 209 m/z – 600 m/z and shorter mass ranges.

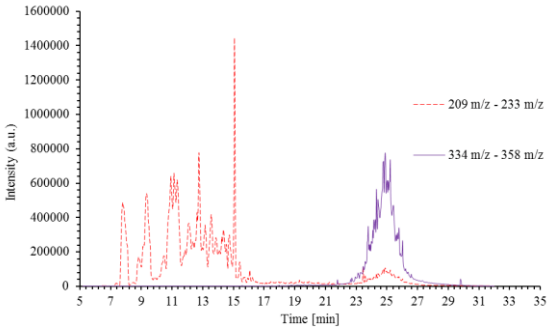

Figure 6 Chromatogram showing response for extracted ion chromatograms (EIC) with mass ranges 209 m/z-233 m/z and 333 m/z-358 m/z. The response of the EIC with mass range 209 m/z-233 m/z at minute 25 is considered as fragments.

There are larger fragments (≥209 m/z) as well, as shown in Figure 6. From the EIC mass ranges (Figure 5), it was determined that the elution of increasing acid masses starts and completes at specific times. As an example, in Figure 6 the acids in the mass range 209 m/z - 233 m/z were found to elute from 7.5 min - 17 min. Consequently, all signal responses from this mass range above 17 minutes were disregarded as small fragments from larger acids or as non-acid molecules. Based on the elution humps for different EIC mass ranges shown in Figure 5, the total chromatogram was split into time segments with increasing minimum m/z cutoffs shown in Table 4, before the intensity averages of each time segment was normalized and summed up to reconstruct the mass distribution for the whole chromatogram. The mass distributions did however, end up looking similar, which indicates that most fragments were found in the mass range 159-208 m/z and that the commercial NA mixture contains mainly low molecular weight acids that when derivatized with

MTBSTFA do not produce high amounts of fragments with higher mass than 209 m/z.

Table 4 Table showing how the chromatogram segments were considered to ensure that fragments did not skew the mass distribution in favor of lower molecular weight acids

Chromatogram segment	Minimum m/z cutoff
7.5 min - 17 min	209
17 min - 22 min	233
22 min - 24 min	258
24 min – 27 min	283
27 min – 29 min	308
29 min – 32 min	333

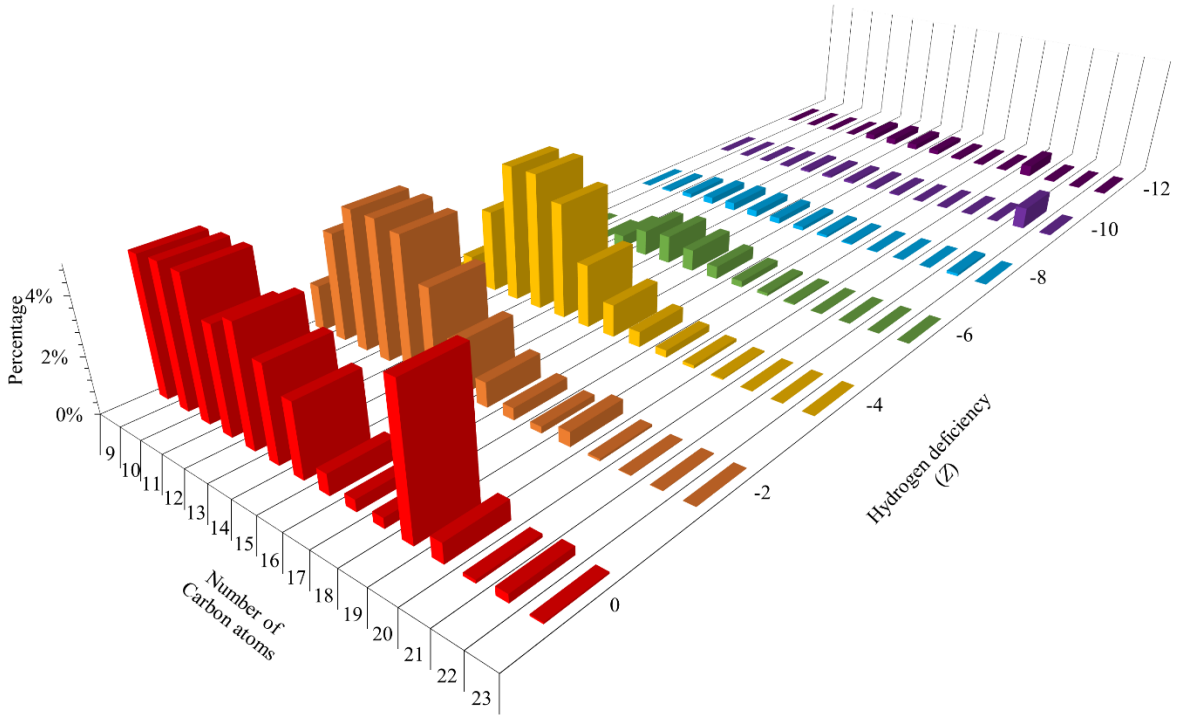

Figure 7 Mass distribution of commercial NA mixture. An attempt to reduce the effects of fragmentation was performed by splitting up the mass spectrums with different mass ranges (Table 4) before recombination (see the text for details). Untreated distribution was not significantly different.

Figure 7 shows that the commercial naphthenic acid mixture consists mainly of aliphatic (Z = 0) and alicyclic structures (Z > -8). The distribution is narrow with regards to carbon numbers and hydrogen deficiency, with C_9 – C_{19} and 0-3 ring structures. Indeed, there are nearly no acids with Z=-8 which is the hydrogen deficiency corresponding to a single aromatic ring or 4 ring structures. This result is consistent with the NMR spectra in Figure 1 and Figure 2. The biggest proportion of peaks seems to fall in the C_9 – C_{15} and 0-2 ring range, although a second mode at C_{19} can be observed, in agreement with the chromatogram presented in Figure 4 . The peaks seen at Z = -12 are most likely a measurement artifact. Indeed, it can be seen in Table 1 that due to the isotopic composition of C and Si, peaks at [M+57]+2 are present in the mass spectrum with an intensity around 5-9% of the stable ion fragment peak [M+57]. Consequently, owing to the periodic structure of Table S1, the peaks at Z = -12 could just correspond to [M+57]+2 isotopes of [M+57] species with Z = 0. The number average molecular weight calculated from the GC/MS mass distribution was 210 g/mol. A comparison of average molecular weight determined by different methods show that this number is lower than the average molecular weight determined by elemental analysis or acid number as seen in Table 5. This could be attributed to lower response factors of higher molecular weight compounds. It must be mentioned that different separation conditions were tested by varying the GC temperature program which all provided similar NA distributions. A well-defined double peak at 387 m/z (C_{22} Z=-10) was observed in the chromatogram. This compound would partition into water at any pH, including acidic ones. Consequently, it is thought that this compound is not a carboxylic acid although it likely contains some functional group which reacts with MTBSTFA since it disappeared when the commercial NA mixture was injected without derivatization agent. By taking the total intensity as the sum of all intensities from 209 m/z to 600 m/z the masses in Table S1 representing the isomer $C_nH_{2n+Z}O_2$ accounted for 80% of the total intensities registered. Using another table with [M+57]+1 m/z due to the isotopes of silicon and carbon accounts for 18% of the total intensities. The remaining 2% falls outside the masses in Table S1 and was considered either an uncertainty or a contribution from phenols [50] or molecules containing oxygen, nitrogen or sulphur groups which do not react with MTBSTFA. It should be mentioned that matching nominal masses could encompass a large amount of different structures, as seen in Table S1 every other mass is counted as an acid when above 259 m/z. This would exclude some naphthenic acids, nitrogen combinations

as these would get an even nominal mass. However, the larger proportion of naphthenic acids with added oxygen, sulphur or other nitrogen functional groups would get odd stable mass fragments so close to the ones in Table S1, that they could not be distinguished with the available precision. However, with the low values for sulphur and nitrogen from the elemental analysis and the assumption that commercial acid mixtures contains few O_3 and O_4 species [10], we still presume to compare our results with the findings of more precise MS analysis on the same commercial NA mixture. Lo, Brownlee and Bunce [46] and Rudzinski, Oehlers, Zhang and Najera [14] examined a commercial NA mixture from Fluka by ESI-MS without prior fractionation to obtain a mass distribution with a large presence of unsaturated compounds filling out hydrogen deficiency columns up to Z = -12, much different from the distribution shown in Figure 7. On the other hand, Hindle, Noestheden, Peru and Headley [47] using HPLC TOF HRMS obtained a completely different distribution from the two previous studies, which does seems to completely overlap with the distribution in Figure 7. This discrepancy in distributions is most likely due to the aforementioned differences between commercial acid mixtures of the same vendor, although part of it could be attributed to the differences seen in analysis with and without chromatographic separation prior to the MS detection [77]. Merlin, Guigard and Fedorak [36] analyzed a commercial NA mixture from the same vendor with GC/MS and MTBSTFA. The article reported the abundance of three mass fragments C_{13} Z=-4 m/z = 267, C_{13} Z =−6 m/z = 265 and C_{14} Z=−6 m/z = 279 with abundances of 9%, 1% and 1% of total ions respectively. As can be seen in Figure 7, our results show abundances of 6%, 1% and 1% of the same mass fragments which is consistent with Merlin, Guigard and Fedorak [36].

Table 5 Summary of results obtained by characterization of the commercial NA mixture.

Method	Average molecular weight
Elemental analysis	226 g/mol
Titration	231 g/mol
GC/MS	210 g/mol

4.2. Determination of the partition ratio

Commercial NA mixture in toluene were shaken in presence of aqueous buffers and the separated phases were derivatized and analyzed with GC/MS. The partition ratio of naphthenic acids was studied using toluene as the oil phase solvent. Choice of the model solvent is not trivial since different equilibria such as dimerization[78] are influenced by the polarity of the solvent. Aromatic solvents have been used in numerous studies as model solvent for crude oil to study compounds like asphaltenes and resins [79] [80, 81]. The extracted ion chromatograms(EIC) between 209 m/z and 600 m/z of derivatized naphthenic acids were extracted from the total ion chromatograms (originally the mass range 159 m/z – 600 m/z was chosen as this correspond to the smallest acids listed in Table S1, however as mentioned in the previous section the masses which registered as acids below C_9 were thought to be smaller fragments due to their constant elution over the entire acid hump). The area under the chromatogram was used to build calibration curves after recombination with the area of the internal standard peak.

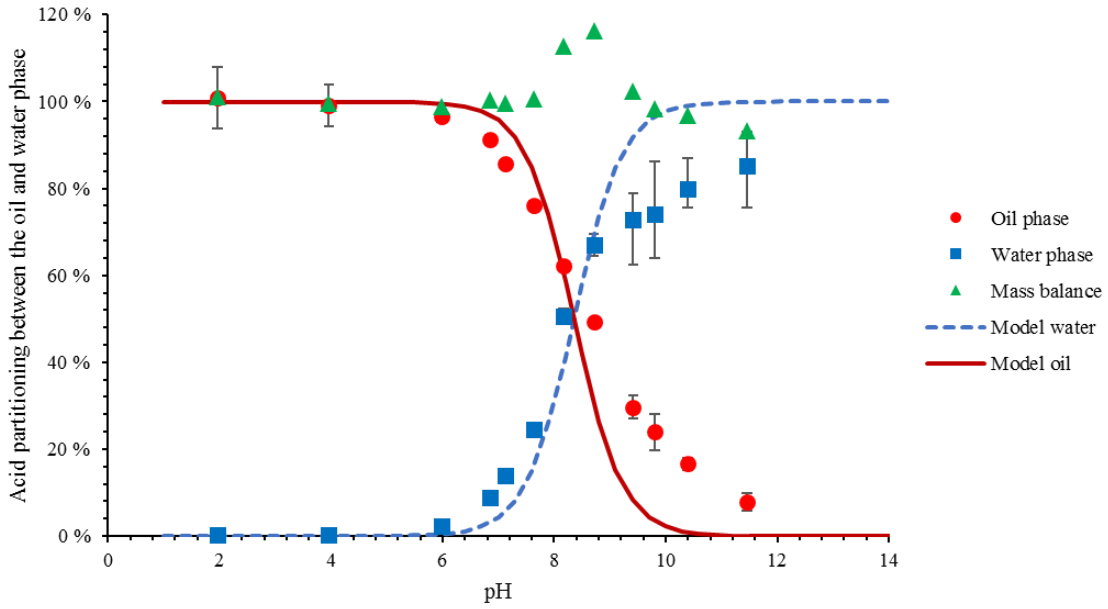

Figure 8 Equilibrium partitioning of the 209 m/z - 600 m/z fraction given as a function of equilibrium pH. The total concentration of the commercial NA mixture was 10 mM or 4 mM for pH higher than 9. Aqueous buffers (3.5wt.% NaCl) were used as water phase. Data was fitted with Equations 5 and 6. The values are the average of two or three measurements where the error bars represent the range of obtained values. Some of the error bars are smaller than the symbols. The mass balance error bars are not specified for clarity's sake.

The equilibrium partitioning for the commercial acid mixture is shown in Figure 8. At low pH values all the acids have a low affinity for the water phase. At pH 6 partitioning starts and at the highest pH value, pH 11.5 around 8% of the acids remain in the oil phase. The pH at which 50% of the naphthenic acids are in water and 50% of the naphthenic acids are in the oil phase is close to 8.4. As pK_a for carboxylic acids and naphthenic acids have been found to have a pK_a between 4 and 6 [42, 54, 82], the pK_a in these calculations has been fixed to a value of 5. From the partitioning equations offered in several papers [59, 60, 83], it can be deduced the apparent pK_a', i.e. the point where the acid(s) is/are equally distributed between the two phases, is equal to the sum of pP_{wo} and pK_a as shown in Equation 9.

$$pK_a' = pK_a + pP_{wo} \quad (9)$$

Headley, Peru, McMartin and Winkler [31] in researching how pH affected solid phase extraction (SPE) recoveries of naphthenic acids from water, agitated a commercial NA mixture from Fluka in various aqueous buffers. The extraction recovery by SPE was reported to 100% at pH 3, 63% at pH 7 and 50% at pH 9, which matches the results obtained in Figure 8 assuming close to 100% of the acids in the water phase are dissociated.

Equations 5 and 6 predicts a pP_{wo} of 3.4 which gives an apparent pK_a' of 8.4, which technically is the point where phase transfer is predominant. However, compared to sharp phase transfers of single compounds [59] the phase transfer of a polydisperse acid mixture happens on a much wider pH range. Consequently, Equations 5 and 6 does not give an accurate fit for the partitioning as a function of pH with a single pP_{wo}.

To obtain an equation to model the partitioning of the polydisperse mixture, it was decided to divide the chromatogram into range fractions to obtain narrower molecular weight ranges. This strategy is similar to the one adopted to obtain the commercial NA mixture carbon numbers and hydrogen deficiency distribution in Figure 7. Indeed, the distribution of the naphthenic acids present in the water phase after partitioning at pH 8 (Figure S1) shows that the lowest molecular weight acids are preferentially partitioned into the aqueous phase. The retention times and the mass range of the different fractions are summarized in Table 6. It must be pointed out that this table is consistent with Table 4. A calibration curve was built for every fraction considered in Table 6, normalized by the internal standard. The signal

obtained from mass ranges above 358 m/z were small and did not yield accurate enough data. Although individual response factors were not used the data should still be regarded as quantitative, as separate calibration curves were built for every fraction, reducing the impact of lower response factors with molecular weight.

*Table 6 Mass ranges considered for quantitative partition analysis of extracted ion chromatograms(EIC's) of the commercial NA mixture and the elution time segment considered to be whole acids and not fragments. *Masses included in the mass ranges are based on naphthenic acid masses [M+57] from Table S1 including their isotope [M+57]+1.*

EIC mass fragment range* [m/z]	Integrated time interval of EIC	R^2 linear range 0.4 mM-15 mM 0.092 g/L-3.4 g/L	Chromatogram area %
209-600	7.5 min – 32 min	0.998	100%
209-233	7.5 min - 17 min	0.997	16 %
234-258	10 min - 22 min	0.999	26 %
259-283	14 min - 24 min	0.999	21 %
284-308	12 min – 27 min	0.999	12 %
309-333	15 min – 29 min	0.997	5 %
334-358	18 min – 30 min	0.995	9 %

In total the areas used for concentration determination of the different fractions encompassed 90% of the total chromatogram area spanning from 209 m/z to 600 m/z. The lacking 10% can be attributed to non-included fragment humps as seen in Figure 6 and masses above 358 m/z.

The equilibrium partitioning of the mass range 209 m/z - 233 m/z is shown in Figure 9. As seen in Table S1 this mass range corresponds to C_9/C_{10} acids. The EIC intensity of this fraction comprises 16% of the total chromatogram area. The acids in this mass range are completely oil soluble below pH 6 and transfer completely to the water phase from pH 6 to 9. Equations 5 and 6 gives an adequate fit with the data when the pP_{wo} is 2.3, indicating that the molecular weight range is narrow enough to be modeled by a single pP_{wo}. However, the mass balance is quite noisy in this mass segment. The apparent pK_a' indicates a phase transfer from pH 7.3.

The equilibrium partitioning of the mass range 234 m/z - 258 m/z, corresponding to C_{11}/C_{12} acids, is shown in Figure 10. The EIC intensity of this fraction comprises 26% of the total chromatogram area. Equations 5 and 6 give a good fit with the data when the pP_{wo} is 2.9 (higher than the value found for the mass range 209-233 m/z) which indicates a phase transfer at the apparent pK_a' of 7.9.

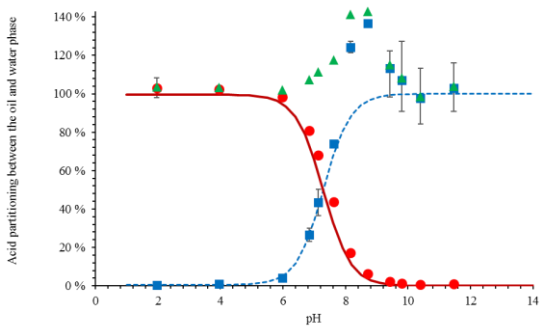

Figure 9 Equilibrium partitioning of the 209 m/z - 233 m/z fraction given as a function of equilibrium pH. The total concentration of the commercial NA mixture was 10 mM or 4 mM for pH higher than 9. Aqueous buffers (3.5wt.% NaCl) were used as water phase. Data was fitted with Equations 5 and 6. The values are the average of two or three measurements where the error bars represent the range of obtained values. Some of the error bars are smaller than the symbols. The mass balance error bars are not specified for clarity's sake.

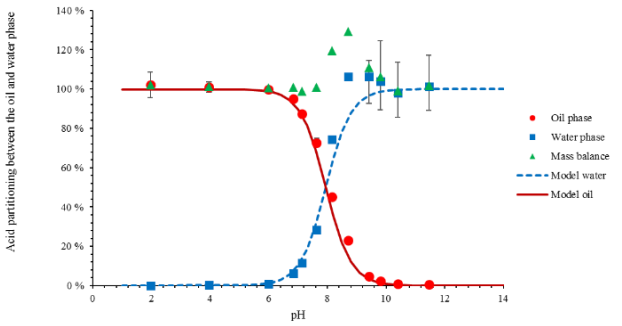

Figure 10 Equilibrium partitioning of the 234 m/z - 258 m/z fraction given as a function of equilibrium pH. The total concentration of the commercial NA mixture was 10 mM or 4 mM for pH higher than 9. Aqueous buffers (3.5wt.% NaCl) were used as water phase. Data was fitted with Equations 5 and 6. The values are the average of two or three measurements where the error bars represent the range of obtained values. Some of the error bars are smaller than the symbols. The mass balance error bars are not specified for clarity's sake.

The equilibrium partitioning of the mass ranges 259 m/z -283 m/z and 284 m/z -308 m/z are shown in Figure 11 and Figure 12. These mass ranges correspond to C_{13}/C_{14} acids and C_{15}/C_{16} acids respectively and likewise comprise 21% and 12% of the total chromatogram area. A good fit with a pP_{wo} of 3.7 is obtained for mass range 259 m/z -283 m/z which gives an apparent pK_a' that indicates a phase transfer at pH 8.7 as seen in Figure 11. Equations 5 and 6 gives a good fit with the data for mass range 284 m/z -308 m/z when the pP_{wo} is 4.7 indicating a phase transfer at pH 9.7.

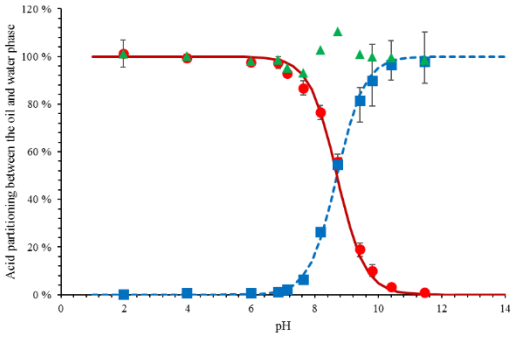

Figure 11 Equilibrium partitioning of the 259 m/z - 283 m/z fraction given as a function of equilibrium pH. The total concentration of the commercial NA mixture was 10 mM or 4 mM for pH higher than 9. Aqueous buffers (3.5wt.% NaCl) were used as water phase. Data was fitted with Equations 5 and 6. The values are the average of two or three measurements where the error bars represent the range of obtained values. Some of the error bars are smaller than the symbols. The mass balance error bars are not specified for clarity's sake.

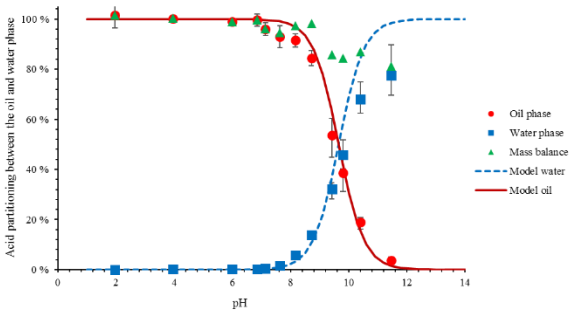

Figure 12 Equilibrium partitioning of the 284 m/z - 308 m/z fraction given as a function of equilibrium pH. The total concentration of the commercial NA mixture was 10 mM or 4 mM for pH higher than 9. Aqueous buffers (3.5wt.% NaCl) were used as water phase. Data was fitted with Equations 5 and 6. The values are the average of two or three measurements where the error bars represent the range of obtained values. Some of the error bars are smaller than the symbols. The mass balance error bars are not specified for clarity's sake.

The equilibrium partitioning of the mass ranges 309 m/z -333 m/z and 334 m/z -358 m/z are shown in Figure 13 and Figure 14. These mass ranges correspond to C_{17} acids and C_{18}/C_{19} acids respectively and likewise comprise 5% and 9% of the total chromatogram area. An adequate fit with a pP_{wo} of 5.2 is obtained for mass range 309 m/z -333 m/z which gives an apparent pK_a' indicating a phase transfer at pH 10.2 as seen in Figure 13. Equations 5 and 6 do not give a good fit with the data for mass range 334 m/z -358 m/z due to incomplete partitioning. The obtained pP_{wo} of 6.7 does not accurately predict the system behavior at high pH. The pP_{wo} values will be further discussed in Figure 16.

The mass balances were systematically determined for all the systems tested and reported in Figure 8 to Figure 14. This mass balance is generally close to 100 % except in two specific situations.

First, at high pH and for higher molecular weight (Figure 13 and Figure 14), the mass balance is lower than 100 %. Here incomplete mass balances at high pH values can be observed which contribute uncertainty to model predictions. Two explanations can be attributed to this loss. The surface activity of naphthenic acids increases with pH as shown by Havre, Sjöblom and Vindstad [42] with interfacial tension studies on the same commercial acid mixture used in this article. The

increased surface activity means more naphthenic acids are present at the interface. However, the surface between oil and water is low (a few cm^2) and therefore the mass present at the interface should represent a negligible part of the total mass of naphthenic acids in the system. Another explanation can be attributed to the slightly opaque water obtained after centrifugation in experiments with initial pH 11 and 12 (pH_f=10.4 and 11.4), where this opaqueness is suspected to be the cause of the sample loss. It was impossible to improve the separation. It was attempted to dissolve 4 mM of pure commercial NA mixture in 3.5wt.% NaCl at pH 12 (pHf=11.4) by shaking overnight. Part of the naphthenic acid mixture did not solubilize and therefore the turbidity seen at high pH in partitioning experiments are most likely attributed to sodium naphthenate particles, which is consistent with the low mass balance. This precipitation of sodium naphthenate is not predicted in the model tested in this article. This should be considered in the prediction for high molecular weight naphthenic acids at high pH for better prediction.

Secondly, the mass balance could be higher than 100 % at intermediate pH (ca. 8) as seen in Figure 9 and Figure 10. Multiple experiments including the testing of different solvents for the back-extraction procedure, building up the calibration curve several times, testing the repeatability, were performed to obtain a better mass balance, but these attempts were unsuccessful. We do not have explanation concerning this discrepancy but we can notice this only concern a few points. This point should be investigated further to improve the accuracy of the method.

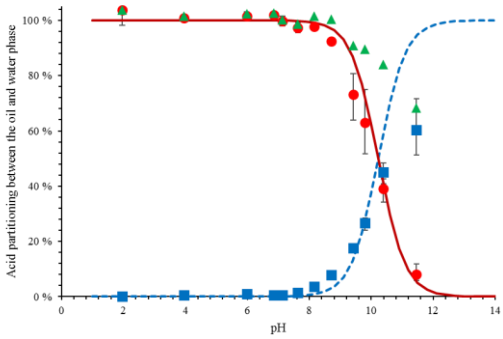

Figure 13 Equilibrium partitioning of the 309 m/z - 333 m/z fraction given as a function of equilibrium pH. The total concentration of the commercial NA mixture was 10 mM or 4 mM for pH higher than 9. Aqueous buffers (3.5wt.% NaCl) were used as water phase. Data was fitted with Equations 5 and 6. The values are the average of two or three measurements where the error bars represent the range of obtained values. Some of the error bars are smaller than the symbols. The mass balance error bars are not specified for clarity's sake.

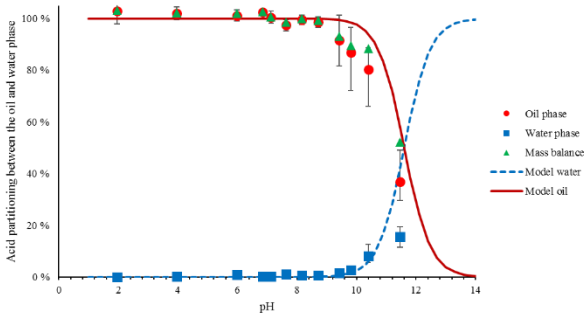

Figure 14 Equilibrium partitioning of the 334 m/z - 358 m/z fraction given as a function of equilibrium pH. The total concentration of the commercial NA mixture was 10 mM or 4 mM for pH higher than 9. Aqueous buffers (3.5wt.% NaCl) were used as water phase. Data was fitted with Equations 5 and 6. The values are the average of two or three measurements where the error bars represent the range of obtained values. Some of the error bars are smaller than the symbols. The mass balance error bars are not specified for clarity's sake.

The mass ranges above 358 m/z correspond to only 3% of the total chromatogram area and do not appear to partition into the water phase. The total naphthenic acid concentration in oil and water can be determined by doing the summation of every individual fraction in proportion to their ratios of the total chromatogram area as seen in Equation 10 and 11. Here the ω_i and $P_{wo,acid,i}$ are the chromatogram area fraction and partition ratio for each mass range respectively.

$$[HA]_{w,tot} = \sum_{i=1}^{n} \omega_i \frac{[HA]_{o,init}}{\frac{[H^+]}{P_{wo,acid,i}(K_{a,HA}+[H^+])}+\frac{V_w}{V_o}} \quad (10)$$

$$[HA]_{o,tot} = \sum_{i=1}^{n} \omega_i \frac{[HA]_{o,init}}{1+\frac{V_w P_{wo,acid,i}(K_{a,HA}+[H^+])}{V_o[H^+]}} \quad (11)$$

This summation model fits the partitioning data of the entire commercial NA mixture perfectly as seen in Figure 15.

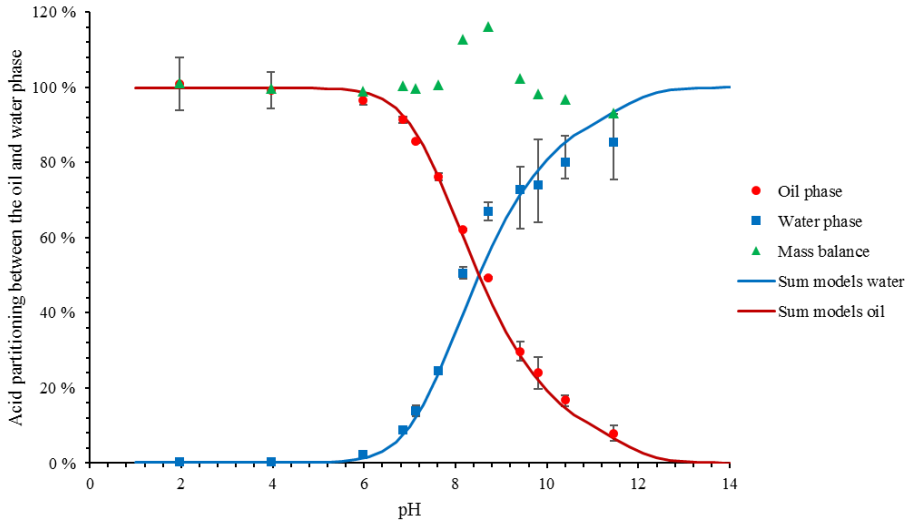

Figure 15 Equilibrium partitioning of the 209 m/z - 600 m/z fraction given as a function of equilibrium pH. The total concentration of the commercial NA mixture was 10 mM or 4 mM for pH higher than 9. Aqueous buffers (3.5wt.% NaCl) were used as water phase. Data was fitted with Equations 10 and 11. The values are the average of two or three measurements where the error bars represent the range of obtained values. Some of the error bars are smaller than the symbols. The mass balance error bars are not specified for clarity's sake.

The findings for the partitioning of the commercial NA mixture are summarized in Table 7. Here the pP_{wo} and apparent pK_a' can be seen to progressively increase with the size of the acids. With few or no aromatic groups in the acid mixture this size increase can only increase the hydrophobic surface area, lowering the water solubility [28, 51]. The increasing molecular weight of acids in the water phase with pH is also found in the experimental findings of Hemmingsen, Kim, Pettersen, Rodgers, Sjöblom and Marshall [15]. This can also be observed in Figure 16, where the linear relationship between molecular weight and pP_{wo} seen before in Reinsel, et al. [84] and Havre, Sjöblom and Vindstad [42] work is expanded. The meaning of the pP_{wo}, the variation with molecular weight, and their comparison with model components will be discussed in the part two article of this study.

Havre et al have determined the CMC of a commercial NA mixture from Fluka at pH = 11.3 and found a value of 0.8 mM. This means that micelles could be formed in some of our systems if the concentration of acids in aqueous phase is higher than this value. The formation of micelles is not considered into the model presented in Equations 5 and 6. By considering the small chromatograms areas of the lowest concentrations considered in the calibration curves, partitioning experiments with similar concentrations under the CMC were deemed unreliable.

*Table 7 Mass ranges and equivalent molecular weight shown in with their respective pP_{wo} calculated by imposing pK_a =5 in Equations 5 and 6. The area fraction of the elution hump of each mass range is also indicated. * pK_a = 5 imposed for naphthenic acids in all mass ranges. ** pP_{wo} calculated on incomplete partitioning in water at high pH. *** Elution hump area do not add to 100% due to fragments registering as naphthenic acids as can be seen in Figure 6.*

Mass range	Molecular weight	Approximate carbon numbers	pK_a*	pP_{wo}	Chromatogram area %	pK_a'
209 – 233 m/z	152 – 176 g /mol	C_9/C_{10}	5	2.3	16 %	7.3
234 – 258 m/z	177 – 201 g/mol	C_{11}/C_{12}	5	2.9	26 %	7.9
259 – 283 m/z	202 – 226 g/mol	C_{13}/C_{14}	5	3.7	21 %	8.7
284 – 308 m/z	227 – 251 g/mol	C_{15}/C_{16}	5	4.7	12 %	9.7
309 – 333 m/z	252 – 276 g/mol	C_{17}	5	5.2	5 %	10.2
334– 358 m/z	277 – 301 g/mol	C_{18}/C_{19}	5	6.6**	9 %	11.6
>359 m/z	>302 g/mol	$>C_{19}$	No partitioning at pH 12		3%	
209-600 m/z	152-543 g/mol		5	3.4	100%***	8.4

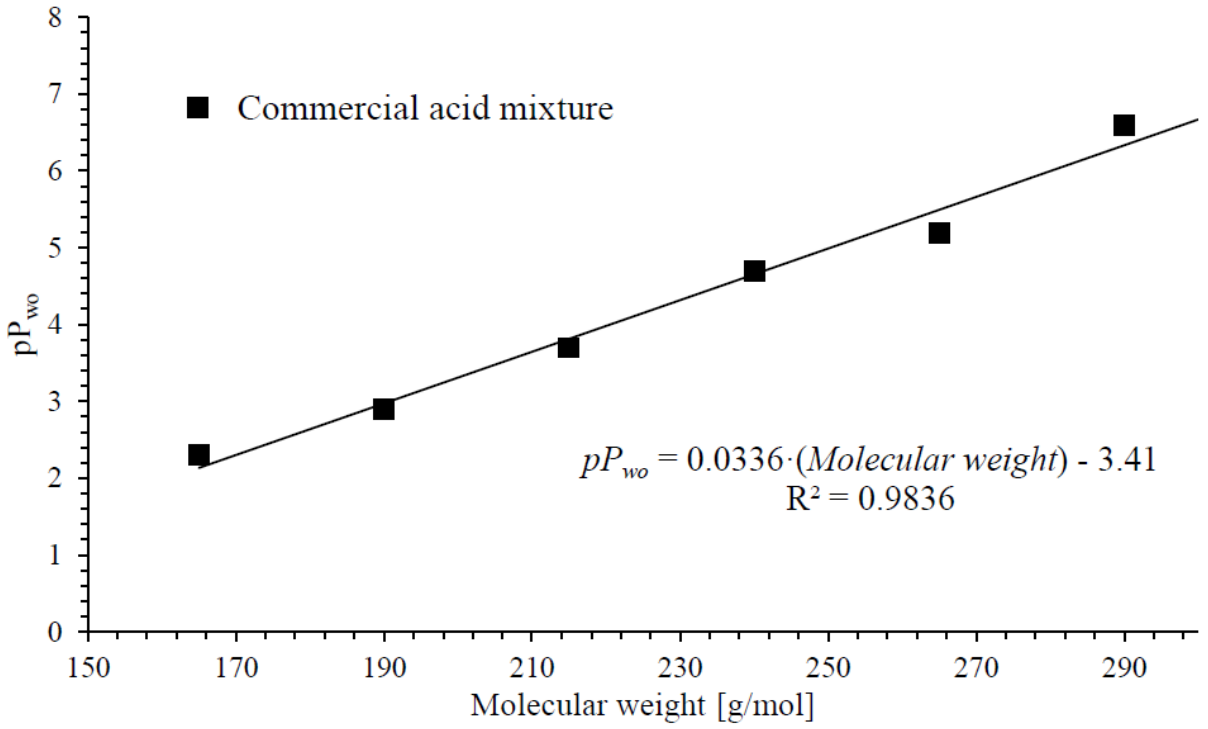

Figure 16 Graph indicating the linearity of the partition ratio pP_{wo} of acid mass ranges from the commercial NA mixture based on molecular weight. The molecular weight indicated corresponds to the middle of the mass ranges.

4.3. Influence of divalent cation on partitioning

As seen in previous work [59] addition of 10 mM divalent cation like calcium to the water phase affected the partitioning of the larger tested acid 4-heptylbenzoic acid with the precipitation of calcium naphthenate CaA_2 at pH 7 and higher, whereas no

significant difference was seen for the partitioning of the small tested acid, phenylacetic acid. To map how calcium would affect the partitioning of a polydisperse mixture of acids, the same experimental setup used in section 4.2 was repeated with the exception that 10 mM $CaCl_2$ was added to the water phase. As mentioned the separated water phases from the experiments with the two highest pH values in section 4.2 in absence of $CaCl_2$, were slightly opaque indicating the presence of colloids such as emulsions or particles. No opaqueness in the separated oil or water phases was observed in the partitioning experiments with calcium. In Figure 17, we see the overall effect of calcium on the whole acid mass range from 209 m/z – 600 m/z. It can be observed that at lower pH values the acid partitioning seems unaffected, whereas a reduction in partitioning can be observed at higher pH values. As the aqueous and oil phase at this pH were not turbid, the presence of precipitated calcium naphthenate can be ruled out. Influence of calcium on high pH oil water mixtures was also reported by Dudek, et al. [85] where it was found to exert a stabilizing effect on oil in water emulsions. This is believed to be caused by calcium complexes or oil soluble calcium naphthenates. Oil soluble calcium naphthenates are discussed by [56, 61, 86].

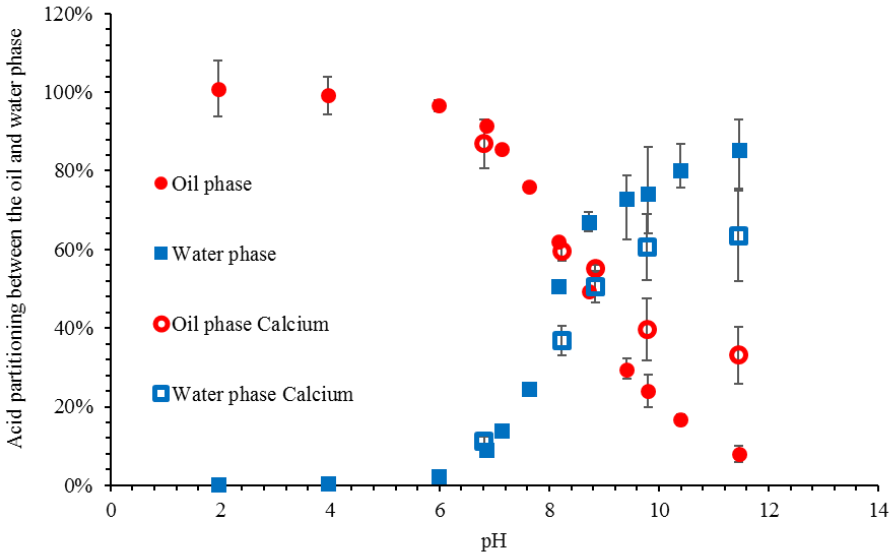

Figure 17. Equilibrium partitioning of the 209 m/z - 600 m/z fraction given as a function of equilibrium pH. The total concentration of the commercial NA mixture was 10 mM or 4 mM for pH higher than 9. Aqueous buffers with 3.5wt.% NaCl or 10 mM $CaCl_2$ and 3.5wt.% NaCl were used as water phase. The values are the average of two or three measurements where the error bars represent the range of obtained values. Some of the error bars are smaller than the symbols. For clarity figures without mass balances are presented here. Figures with mass balances are presented in the supporting information.

To study this in more detail the mass ranges were considered individually to see how calcium affected different naphthenic acid sizes. As seen in Figure 18 and Figure 19 which present the partitioning of the mass ranges 209 m/z-233 m/z (C_9/C_{10}) and 234 m/z-258 m/z (C_{11}/C_{12}), the smaller naphthenic acids are largely unaffected by the presence of calcium as was the case for the small model acid, phenylacetic acid (which would have a stable mass fragment of 193 m/z) in a previous article[59].

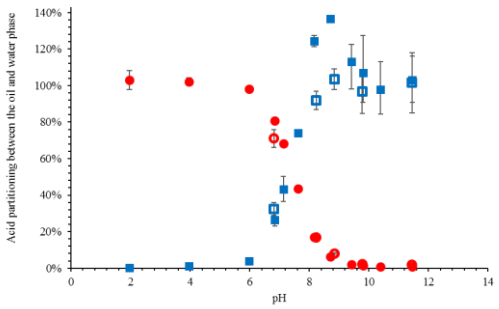

Figure 18 Equilibrium partitioning of the 209 m/z - 233 m/z fraction given as a function of equilibrium pH. The total concentration of the commercial NA mixture was 10 mM or 4 mM for pH higher than 9. Aqueous buffers with 3.5wt.% NaCl or 10 mM $CaCl_2$ and 3.5wt.% NaCl were used as water phase. The values are the average of two or three measurements where the error bars represent the range of obtained values. Some of the error bars are smaller than the symbols. For clarity figures without mass balances are presented here. Figures with mass balances are presented in the supporting information.

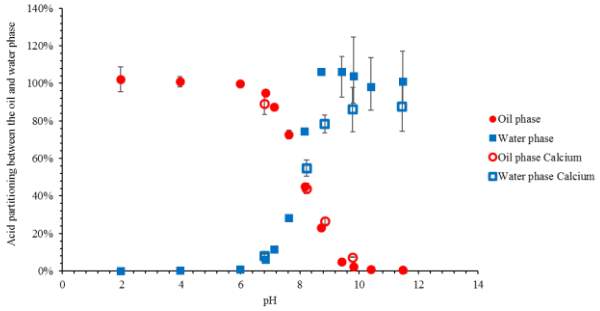

Figure 19 Equilibrium partitioning of the 234 m/z - 258 m/z fraction given as a function of equilibrium pH. The total concentration of the commercial NA mixture was 10 mM or 4 mM for pH higher than 9. Aqueous buffers with 3.5wt.% NaCl or 10 mM $CaCl_2$ and 3.5wt.% NaCl were used as water phase. The values are the average of two or three measurements where the error bars represent the range of obtained values. Some of the error bars are smaller than the symbols. For clarity figures without mass balances are presented here. Figures with mass balances are presented in the supporting information.

Figure 20 a-d compare the acid partitioning with and without calcium present for the remaining mass ranges 259 m/z - 283 m/z (C_{13}/C_{14}), 284 m/z - 308 m/z (C_{15}/C_{16}), 309 m/z - 333 m/z (C_{17}) and 334 m/z - 358 m/z (C_{18}/C_{19}). At low pH values calcium still does not affect the partitioning. At higher pH values the partitioning is reduced as the molecular weight of the acids increases. A stable mass balance (as can be observed in Figure S2 in the supporting information) also indicates little or no loss of sample due to precipitation of calcium naphthenate particles, as confirmed by visual inspection of the samples after centrifugation, no visible turbidity or particles. The difference in partitioning between systems with and without calcium could come from either a salting out effect from $CaCl_2$ or the presence of oil-soluble calcium naphthenates. Indeed, it has been previously recorded that calcium preferentially forms oil soluble calcium naphthenate with higher molecular weight acids [86].

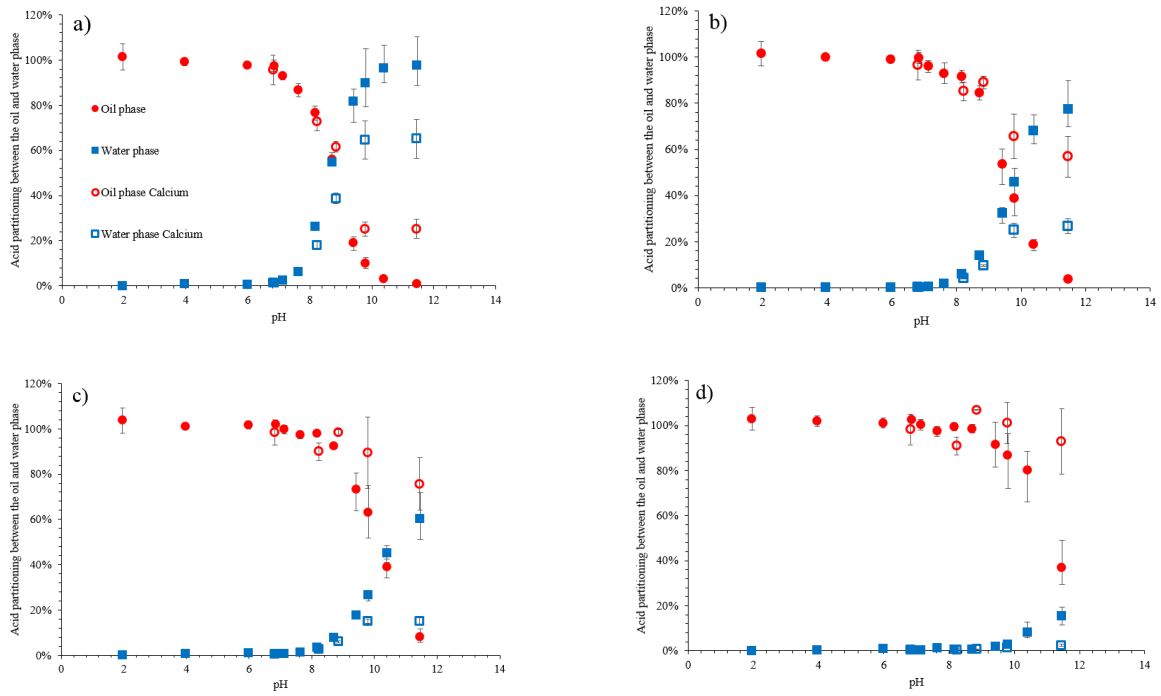

Figure 20 Equilibrium partitioning of the fractions (a) 259 m/z - 283 m/z, (b) 284 m/z - 308 m/z, (c) 309 m/z - 333 m/z, (d) 334 m/z - 358 m/z given as a function of equilibrium pH. The total concentration of the commercial NA mixture was 10 mM or 4 mM for pH higher than 9. Aqueous buffers with 3.5wt.% NaCl or 10 mM $CaCl_2$ and 3.5wt.% NaCl were used as water phase. The values are the average of two or three measurements where the error bars represent the range of obtained values. Some of the error bars are smaller than the symbols. For clarity figures without mass balances are presented here. Figures with mass balances are presented in the supporting information.

To determine which explanation is the most likely, the elemental composition, especially calcium content of the oil phase after evaporation of toluene was determined at three different pH values (2, 10 and 12) as seen in Table 8. The samples were all prepared in duplicates and analyzed. The table shows that the compositions are slightly different between the two parallels, but the trends are reproducible. The composition at low pH is relatively like that of the commercial NA mixture since negligible partitioning takes place at this pH. At higher pH the percentage of oxygen decreases which could be attributed to an increase of the molecular weight of the naphthenic acid in oil phase. This increase is consistent with the variation of the pP_{wo} with molecular weight. At high pH the carbon over oxygen

ratio indicated a high average carbon number varying C_{33} to C_{66} depending on the pH and the parallel, i.e. bigger than the largest molecule present in the Fluka naphthenic acid mixture (see Figure 7). These surprising values are difficult to explain, and could result from the possible presence of neutral impurities present in the Fluka naphthenic acid samples, these impurities would be more preponderant in the elemental analysis at high pH because most of the naphthenic acids would have partitioned into the water phase.

The ratio between the moles of oxygen and calcium was calculated to determine the number of calcium atoms per carbonyl group. The results show that around pH 10 only half of the carbonyl groups in the oil are bound to calcium (note that 2 $RCOO^-$ are needed per Ca^{2+}), while at higher pH all the carbonyl groups in the oil phase are bound to calcium. This effect is likely caused by higher degree of acid dissociation at higher pH.

Table 8 Elemental composition of evaporated oil phase acids after shaken to equilibrium with pH 2, 10 and 12 buffers with 3.5% NaCl and 10 mM $CaCl_2$. The / bar separates the results of the analysis of two independently prepared samples.

Final pH	**Carbon [%]**	**Hydrogen [%]**	**Oxygen [%]**	**Calcium [%]**	**Sodium [%]**	**Chlorine [%]**	**Mol $\frac{\text{Calcium}}{\text{Mol COO-}}$**
pH 1.94	75.3/77.1	11.5/12.1	13.1/10.9	<0.01/<0.01	<0.01/<0.01	<0.4/<0.4	≈0
pH 9.8	78.6/82.0	12.4/13.2	6.25/3.31	1.6/0.87	0.03/0.01	<0.4/<0.4	0.21/0.21
pH 11.5	76.4/78.2	11.9/12.5	6.2/4.2	3.7/2.5	0.02/0.02	<0.4/<0.4	0.48/0.46

In summary, it seems that from the mass range 209 m/z - 258 m/z (C_9-C_{12}), calcium does not seem to affect the acid partitioning. On the contrary in the mass range 259 m/z - 358 m/z (C_{13}-C_{19}), calcium reduces the partitioning at high pH, most likely by forming oil soluble calcium naphthenates which is consistent with the composition of calcium in the oil phase.

5. Conclusion

Model acids and a commercial naphthenic acid mixture from Fluka was analyzed by low resolution GC/MS. The derivatization agent produced a dominant stable mass fragment ion for all model acid structures tested. Other ion fragments from predominantly aromatic acids, polycyclic acids and high molecular weight acids in general, would influence the analysis of the commercial naphthenic acid mixture. A method to analyze mass spectra was developed to avoid this pitfall, consisting mostly by dividing up the chromatogram into different mass range fractions. The GC/MS analysis show that the commercial naphthenic acid mixture contains exclusively saturated acids with up to 19 carbon atoms and hydrogen deficiencies from 0 to -6 or 0 to 3 rings structures. The partitioning of the commercial naphthenic acid mixture versus pH was analyzed with GC/MS. The acids had an almost complete partitioning over the pH range 6-12. A model with one partition ratio for the polydisperse acid mixture did not manage to represent the experimental results of the entire naphthenic acid mixture. Consequently, a new method was developed consisting to analyze narrow molecular weight ranges (width: 25 g/mol) to determine their partition ratio pP_{wo}. By summing up contributions from each mass range a model was made which predicted the partitioning of the entire naphthenic acid mixture perfectly. Low mass balance for high molecular weight naphthenic acids indicated the possible precipitation of sodium naphthenate, not considered in the model. Adding calcium to the water phase did not affect partitioning at low pH and reduced the partitioning at high pH. Elemental analysis indicated the likely cause was the formation of oil soluble calcium naphthenates. Calcium seemed to increasingly reduce the partitioning of high molecular weight acids while the partitioning of the smaller acids seemed unaffected. This work has given valuable insight into acid partitioning which will be further explored in the examination of extracted crude oil acids. Future work could include the comparison of the data obtained in this article with pK_a of the naphthenic acids partitioned into water determined by potentiometric titration.

Acknowledgements

This work was carried out as a part of SUBPRO, a Research-based Innovation Centre within Subsea Production and Processing. The authors gratefully acknowledge the financial support from SUBPRO, which is financed by the Research Council of Norway, major industry partners and NTNU. The authors would like to thank Bicheng Gao (NTNU) for the determination of NMR spectra.

Supporting information. Table S1 displaying the naphthenic acid masses for increasing carbon numbers and hydrogen deficiencies. Figure S1 Mass distribution of naphthenic acids in the water phase at pH 8. Figure S2 a-g, graphs showing equilibrium partitioning of naphthenic acids with and without calcium and the mass balances.

References

1. Khoi Vu, V.; Fantoft, R.; Shaw, C. K.; Gruehagen, H., Comparison Of Subsea Separation Systems. In *Offshore Technology Conference*, Houston, Texas, USA, 4-7 May, OTC 20080, 2009.
2. Prescott, C. N., Subsea Separation and Processing of Oil, Gas & Produced Water. Past, Present and Future. Why We Need It Now. In *Rice Global E&C Forum*, Fluor Offshore Solutions: Houston, Texas, 2012.
3. Wenger, L. M.; Davis, C. L.; Isaksen, G. H., Multiple Controls on Petroleum Biodegradation and Impact on Oil Quality SPE-80168-PA. *SPE Reservoir Evaluation & Engineering* **2002,** 5, (5).
4. Barth, T.; Høiland, S.; Fotland, P.; Askvik, K. M.; Myklebust, R.; Erstad, K., Relationship between the Content of Asphaltenes and Bases in Some Crude Oils. *Energy & Fuels* **2005,** 19, (4), 1624-1630.
5. Barth, T.; Høiland, S.; Fotland, P.; Askvik, K. M.; Pedersen, B. S.; Borgund, A. E., Acidic compounds in biodegraded petroleum. *Organic Geochemistry* **2004,** 35, (11–12), 1513-1525.
6. Berntsen, J. S., Qualified technology (TRL 5) to remove produced water, at seafloor or topside, before it becomes difficult to treat. In *Tekna Produced Water Management Conference*, Stavanger, Norway, 2018.
7. Brandal, Ø. Interfacial (o/w) Properties of Naphthenic Acids and Metal Naphthenates, Naphthenic Acid Characterization and Metal Naphthenate Inhibition. PhD thesis, NTNU, Trondheim, Norway, 2005.
8. Shepherd, A. G. A Mechanistic Analysis of Naphthenate and Carboxylate Soap-Forming Systems in Oilfield Exploration and Production. PhD thesis, Heriot-Watt University, Edinburg, UK, 2008.
9. Headley, J. V., McMartin, Dena W., A Review of the Occurrence and Fate of Naphthenic Acids in Aquatic Environments. *Journal of Environmental Science and Health Part A* **2004,** A39, (8), 1989–2010.
10. Grewer, D. M.; Young, R. F.; Whittal, R. M.; Fedorak, P. M., Naphthenic acids and other acid-extractables in water samples from Alberta: what is being measured? *Science of the Total Environment* **2010,** 408, (23), 5997–6010.
11. Headley, J. V.; Peru, K. M.; Mohamed, M. H.; Frank, R. A.; Martin, J. W.; Hazewinkel, R. R. O.; Humphries, D.; Gurprasad, N. P.; Hewitt, L. M.; Muir, D. C. G.; Lindeman, D.; Strub, R.; Young, R. F.; Grewer, D. M.; Whittal, R. M.; Fedorak, P. M.; Birkholz, D. A.; Hindle, R.; Reisdorph, R.; Wang, X.; Kasperski, K. L.; Hamilton, C.; Woudneh, M.; Wang, G.; Loescher, B.; Farwell, A.; Dixon, D. G.; Ross, M.; Pereira, A. D. S.; King, E.; Barrow, M. P.; Fahlman, B.; Bailey, J.; McMartin, D. W.; Borchers, C. H.; Ryan, C. H.; Toor, N. S.; Gillis, H. M.; Zuin, L.; Bickerton, G.; Mcmaster, M.; Sverko, E.; Shang, D.; Wilson, L. D.; Wrona, F. J., Chemical fingerprinting of naphthenic acids and oil sands process waters-A review of analytical methods for environmental samples. *Journal of Environmental Science and Health. Part A, Toxic/hazardous Substances & Environmental Engineering* **2013,** 48, 1145-1163.
12. Qian, K.; Robbins, W. K.; Hughey, C. A.; Cooper, H. J.; Rodgers, R. P.; Marshall, A. G., Resolution and Identification of Elemental Compositions for More than 3000 Crude Acids in Heavy Petroleum by Negative-Ion Microelectrospray High-Field Fourier Transform Ion Cyclotron Resonance Mass Spectrometry. *Energy & Fuels* **2001,** 15, (6), 1505-1511.
13. Tomczyk, N. A.; Winans, R. E.; Shinn, J. H.; Robinson, R. C., On the Nature and Origin of Acidic Species in Petroleum. 1. Detailed Acid Type Distribution in a California Crude Oil. *Energy & Fuels* **2001,** 15, (6), 1498-1504.

14. Rudzinski, W. E.; Oehlers, L.; Zhang, Y.; Najera, B., Tandem Mass Spectrometric Characterization of Commercial Naphthenic Acids and a Maya Crude Oil. *Energy & Fuels* **2002,** 16, (5), 1178-1185.
15. Hemmingsen, P. V.; Kim, S.; Pettersen, H. E.; Rodgers, R. P.; Sjöblom, J.; Marshall, A. G., Structural Characterization and Interfacial Behavior of Acidic Compounds Extracted from a North Sea Oil. *Energy & Fuels* **2006,** 20, (5), 1980-1987.
16. Barrow, M. P.; McDonnell, L. A.; Feng, X.; Walker, J.; Derrick, P. J., Determination of the Nature of Naphthenic Acids Present in Crude Oils Using Nanospray Fourier Transform Ion Cyclotron Resonance Mass Spectrometry: The Continued Battle Against Corrosion. *Analytical Chemistry* **2003,** 75, (4), 860-866.
17. Ese, M.-H.; Kilpatrick, P. K., Stabilization of Water-in-Oil Emulsions by Naphthenic Acids and Their Salts: Model Compounds, Role of pH, and Soap : Acid Ratio. *Journal Of Dispersion Science And Technology* **2004,** 25, (3), 253-261.
18. Häger, M.; Ese, M. H.; Sjöblom, J., Emulsion Inversion in an Oil-Surfactant-Water System Based on Model Naphthenic Acids under Alkaline Conditions. *Journal of Dispersion Science and Technology* **2005,** 26, (6), 673-682.
19. Vindstad, J. E.; Bye, A. S.; Grande, K. V.; Hustad, B.; Hustvedt, E.; Nergård, B., Fighting Naphthenate Deposition at the Heidrun Field. In *International Symposium on Oilfield Scale*, Society of Petroleum Engineers: January 29-30th, Aberdeen, UK, SPE 80375, 2003.
20. Sarac, S.; Civan, F., Mechanisms, Parameters, and Modeling of Naphthenate-Soap-Induced Formation Damage. *Society of Petroleum Engineers Journal* **2009,** 14, (2), 259-266.
21. Scarlett, A. G.; West, C. E.; Jones, D.; Galloway, T. S.; Rowland, S. J., Predicted toxicity of naphthenic acids present in oil sands process-affected waters to a range of environmental and human endpoints. *Sci Total Environ* **2012,** 425, 119-27.
22. Li, C.; Fu, L.; Stafford, J.; Belosevic, M.; Gamal El-Din, M., The toxicity of oil sands process-affected water (OSPW): A critical review. *Sci Total Environ* **2017,** 601-602, 1785-1802.
23. Thomas, K. V.; Langford, K.; Petersen, K.; Smith, A. J.; Tollefsen, K. E., Effect-Directed Identification of Naphthenic Acids As Important in Vitro Xeno-Estrogens and Anti-Androgens in North Sea Offshore Produced Water Discharges. *Environmental Science & Technology* **2009,** 43, (21), 8066-8071.
24. St. John, W. P.; Rughani, J.; Green, S. A.; McGinnis, G. D., Analysis and characterization of naphthenic acids by gas chromatography–electron impact mass spectrometry of tert.-butyldimethylsilyl derivatives. *Journal of Chromatography A* **1998,** 807, (2), 241-251.
25. Scott, A. C.; Young, R. F.; Fedorak, P. M., Comparison of GC–MS and FTIR methods for quantifying naphthenic acids in water samples. *Chemosphere* **2008,** 73, (8), 1258-1264.
26. Holowenko, F. M.; MacKinnon, M. D.; Fedorak, P. M., Characterization of naphthenic acids in oil sands wastewaters by gas chromatography-mass spectrometry. *Water Research* **2002,** 36, (11), 2843-2855.
27. Clemente, J. S.; Fedorak, P. M., A review of the occurrence, analyses, toxicity, and biodegradation of naphthenic acids. *Chemosphere* **2005,** 60, (5), 585-600.
28. Stanford, L. A.; Kim, S.; Klein, G. C.; Smith, D. F.; Rodgers, R. P.; Marshall, A. G., Identification of Water-Soluble Heavy Crude Oil Organic-Acids, Bases, and Neutrals by Electrospray Ionization and Field Desorption Ionization Fourier Transform Ion Cyclotron Resonance Mass Spectrometry. *Environmental Science & Technology* **2007,** 41, (8), 2696-2702.
29. Damasceno, F. C.; Gruber, L. D. A.; Geller, A. M.; Vaz de Campos, M. C.; Gomes, A. O.; Guimaraes, R. C. L.; Peres, V. F.; Jacques, R. A.; Caramao, E. B., Characterization of naphthenic acids using mass spectroscopy and chromatographic techniques: study of technical mixtures. *Analytical Methods* **2014,** 6, (3), 807-816.

30. Lewis, A. T.; Tekavec, T. N.; Jarvis, J. M.; Juyal, P.; McKenna, A. M.; Yen, A. T.; Rodgers, R. P., Evaluation of the Extraction Method and Characterization of Water-Soluble Organics from Produced Water by Fourier Transform Ion Cyclotron Resonance Mass Spectrometry. *Energy & Fuels* **2013,** 27, (4), 1846-1855.
31. Headley, J. V.; Peru, K. M.; McMartin, D. W.; Winkler, M., Determination of dissolved naphthenic acids in natural waters by using negative-ion electrospray mass spectrometry. *Journal of AOAC International* **2002,** 85, 182-187.
32. Anderson, K.; Atkins, M. P.; Goodrich, P.; Hardacre, C.; Hussain, A. S.; Pilus, R.; Rooney, D. W., Naphthenic acid extraction and speciation from Doba crude oil using carbonate-based ionic liquids. *Fuel* **2015,** 146, 60-68.
33. Clingenpeel, A. C.; Rowland, S. M.; Corilo, Y. E.; Zito, P.; Rodgers, R. P., Fractionation of Interfacial Material Reveals a Continuum of Acidic Species That Contribute to Stable Emulsion Formation. *Energy & Fuels* **2017,** 31, (6), 5933-5939.
34. Stanford, L. A.; Rodgers, R. P.; Marshall, A. G.; Czarnecki, J.; Wu, X. A.; Taylor, S., Detailed Elemental Compositions of Emulsion Interfacial Material versus Parent Oil for Nine Geographically Distinct Light, Medium, and Heavy Crude Oils, Detected by Negative- and Positive-Ion Electrospray Ionization Fourier Transform Ion Cyclotron Resonance Mass Spectrometry. *Energy & Fuels* **2007,** 21, (2), 973-981.
35. Jones, D. M.; Watson, J. S.; Meredith, W.; Chen, M.; Bennett, B., Determination of Naphthenic Acids in Crude Oils Using Nonaqueous Ion Exchange Solid-Phase Extraction. *Analytical Chemistry* **2001,** 73, (3), 703-707.
36. Merlin, M.; Guigard, S. E.; Fedorak, P. M., Detecting naphthenic acids in waters by gas chromatography–mass spectrometry. *Journal of Chromatography A* **2007,** 1140, (1–2), 225-229.
37. Young, R. F.; Wismer, W. V.; Fedorak, P. M., Estimating naphthenic acids concentrations in laboratory-exposed fish and in fish from the wild. *Chemosphere* **2008,** 73, (4), 498-505.
38. Schummer, C.; Delhomme, O.; Appenzeller, B. M. R.; Wennig, R.; Millet, M., Comparison of MTBSTFA and BSTFA in derivatization reactions of polar compounds prior to GC/MS analysis. *Talanta* **2009,** 77, (4), 1473-1482.
39. Clemente, J. S.; Fedorak, P. M., Evaluation of the analyses of tert-butyldimethylsilyl derivatives of naphthenic acids by gas chromatography–electron impact mass spectrometry. *Journal of Chromatography A* **2004,** 1047, (1), 117-128.
40. Shepherd, A. G.; van Mispelaar, V.; Nowlin, J.; Genuit, W.; Grutters, M., Analysis of Naphthenic Acids and Derivatization Agents Using Two-Dimensional Gas Chromatography and Mass Spectrometry: Impact on Flow Assurance Predictions. *Energy & Fuels* **2010,** 24, (4), 2300-2311.
41. Gutierrez-Villagomez, J. M.; Vázquez-Martínez, J.; Ramírez-Chávez, E.; Molina-Torres, J.; Trudeau, V. L., Analysis of naphthenic acid mixtures as pentafluorobenzyl derivatives by gas chromatography-electron impact mass spectrometry. *Talanta* **2017,** 162, 440-452.
42. Havre, T. E.; Sjöblom, J.; Vindstad, J. E., Oil/Water-Partitioning and Interfacial Behavior of Naphthenic Acids. *Journal of Dispersion Science and Technology* **2003,** 24, (6), 789-801.
43. Ahmed, M. M. Characterization, modelling, prediction and inhibition of naphthenate deposits in oilfield production. PhD thesis, Heriot-Watt University, Edinburgh, UK, 2010.
44. Hsu, C. S.; Dechert, G. J.; Robbins, W. K.; Fukuda, E. K., Naphthenic Acids in Crude Oils Characterized by Mass Spectrometry. *Energy & Fuels* **2000,** 14, (1), 217-223.
45. West, C. E.; Scarlett, A. G.; Pureveen, J.; Tegelaar, E. W.; Rowland, S. J., Abundant naphthenic acids in oil sands process-affected water: studies by synthesis, derivatisation and two-dimensional gas chromatography/high-resolution mass spectrometry. *Rapid Communications in Mass Spectrometry* **2013,** 27, (2), 357-65.

46. Lo, C. C.; Brownlee, B. G.; Bunce, N. J., Mass spectrometric and toxicological assays of Athabasca oil sands naphthenic acids. *Water Research* **2006,** 40, (4), 655-664.
47. Hindle, R.; Noestheden, M.; Peru, K.; Headley, J., Quantitative analysis of naphthenic acids in water by liquid chromatography–accurate mass time-of-flight mass spectrometry. *Journal of Chromatography A* **2013,** 1286, (Supplement C), 166-174.
48. Rowland, S. J.; West, C. E.; Scarlett, A. G.; Jones, D., Identification of individual acids in a commercial sample of naphthenic acids from petroleum by two-dimensional comprehensive gas chromatography/mass spectrometry. *Rapid Communications in Mass Spectrometry* **2011,** 25, (12), 1741-1751.
49. Saab, J.; Mokbel, I.; Razzouk, A. C.; Ainous, N.; Zydowicz, N.; Jose, J., Quantitative Extraction Procedure of Naphthenic Acids Contained in Crude Oils. Characterization with Different Spectroscopic Methods. *Energy & Fuels* **2005,** 19, (2), 525-531.
50. West, C. E.; Jones, D.; Scarlett, A. G.; Rowland, S. J., Compositional heterogeneity may limit the usefulness of some commercial naphthenic acids for toxicity assays. *Sci Total Environ* **2011,** 409, (19), 4125-31.
51. Turner, A., Salting out of chemicals in estuaries: implications for contaminant partitioning and modelling. *Science of The Total Environment* **2003,** 314–316, 599-612.
52. Celsie, A.; Parnis, J. M.; Mackay, D., Impact of temperature, pH, and salinity changes on the physico-chemical properties of model naphthenic acids. *Chemosphere* **2016,** 146, 40-50.
53. Kanicky, J. R.; Shah, D. O., Effect of Premicellar Aggregation on the pKa of Fatty Acid Soap Solutions. *Langmuir* **2003,** 19, (6), 2034-2038.
54. Brient, J. A.; Wessner, P. J.; Doyle, M. N., Naphthenic Acids. In *Encyclopedia of Chemical Technology*, Kirk-Othmer, Ed. John Wiley & Sons, Inc.: New York, 1995; pp 1017-1029.
55. Touhami, Y.; Hornof, V.; Neale, G. H., Mechanisms for the Interactions between Acidic Oils and Surfactant-Enhanced Alkaline Solutions. *Journal of Colloid and Interface Science* **1996,** 177, (2), 446-455.
56. Hurtevent, C.; Bourrel, M.; Rousseau, G.; Brocart, B., Production Issues of Acidic Petroleum Crude Oils. In *Emulsions and Emulsion Stability*, Sjöblom, J., Ed. CRC Press: 2005; pp 477-516.
57. Hutin, A.; Argillier, J.-F.; Langevin, D., Mass Transfer between Crude Oil and Water. Part 1: Effect of Oil Components. *Energy & Fuels* **2014,** 28, (12), 7331-7336.
58. Nordgård, E. L.; Ahmad, J.; Simon, S.; Sjöblom, J., Oil-Water Partitioning of a Synthetic Tetracarboxylic Acid as a Function of pH. *Journal of Dispersion Science and Technology* **2012,** 33, (6), 871-880.
59. Bertheussen, A.; Simon, S.; Sjöblom, J., Equilibrium partitioning of naphthenic acids and bases and their consequences on interfacial properties. *Colloids and Surfaces A: Physicochemical and Engineering Aspects* **2017,** 529, (Supplement C), 45-56.
60. Scherrer, R. A.; Howard, S. M., Use of distribution coefficients in quantitative structure-activity relationships. *J Med Chem* **1977,** 20, (1), 53-8.
61. Cooke, C. E., Jr.; Williams, R. E.; Kolodzie, P. A., Oil Recovery by Alkaline Waterflooding. *Journal of Petroleum Technology* **1974,** 26, (12), 1365-1374.
62. Brandal, Ø.; Sjöblom, J., Interfacial Behavior of Naphthenic Acids and Multivalent Cations in Systems with Oil and Water. II: Formation and Stability of Metal Naphthenate Films at Oil-Water Interfaces. *Journal of Dispersion Science and Technology* **2005,** 26, (1), 53-58.
63. Havre, T. E. Formation of Calcium Naphthenate in Water/Oil Systems, Naphthenic Acid Chemistry and Emulsion Stability. PhD thesis, NTNU, Trondheim, Norway, Trondheim, 2002.
64. Hanneseth, A. M. D.; Brandal, Ø.; Sjöblom, J., Formation, Growth, and Inhibition of Calcium Naphthenate Particles in Oil/Water Systems as Monitored by Means of Near Infrared Spectroscopy. *Journal of Dispersion Science and Technology* **2006,** 27, (2), 185-192.

65. Simon, S.; Reisen, C.; Bersås, A.; Sjöblom, J., Reaction Between Tetrameric Acids and Ca2+ in Oil/Water System. *Industrial & Engineering Chemistry Research* **2012,** 51, (16), 5669-5676.
66. Sjöblom, J.; Simon, S.; Xu, Z., The chemistry of tetrameric acids in petroleum. *Advances in Colloid and Interface Science* **2014,** 205, (0), 319-338.
67. Lide, D. R., CRC handbook of chemistry and physics: A ready-reference book of chemical and physical data. In 77 ed.; CRC Press Inc.: Boca Raton, Florida, US, 1997; p 842.
68. Lu, Y.; Wang, J.; Deng, Z.; Wu, H.; Deng, Q.; Tan, H.; Cao, L., Isolation and characterization of fatty acid methyl ester (FAME)-producing Streptomyces sp. S161 from sheep (Ovis aries) faeces. *Lett Appl Microbiol* **2013,** 57, (3), 200-5.
69. Barros, E. V.; Dias, H. P.; Pinto, F. E.; Gomes, A. O.; Moura, R. R.; Neto, A. C.; Freitas, J. C. C.; Aquije, G. M. F. V.; Vaz, B. G.; Romão, W., Characterization of Naphthenic Acids in Thermally Degraded Petroleum by ESI(−)-FT-ICR MS and 1H NMR after Solid-Phase Extraction and Liquid/Liquid Extraction. *Energy & Fuels* **2018,** In print.
70. ThermoScientific, Reagents, Solvents and Accessories catalogue. In 2012.
71. Acevedo, S.; Escobar, G.; Ranaudo, M. A.; Khazen, J.; Borges, B.; Pereira, J. C.; Méndez, B., Isolation and Characterization of Low and High Molecular Weight Acidic Compounds from Cerro Negro Extraheavy Crude Oil. Role of These Acids in the Interfacial Properties of the Crude Oil Emulsions. *Energy & Fuels* **1999,** 13, (2), 333-335.
72. Mapolelo, M. M.; Rodgers, R. P.; Blakney, G. T.; Yen, A. T.; Asomaning, S.; Marshall, A. G., Characterization of naphthenic acids in crude oils and naphthenates by electrospray ionization FT-ICR mass spectrometry. *International Journal of Mass Spectrometry* **2011,** 300, (2–3), 149-157.
73. Wang, Z.; Hollebone, B. P.; Fingas, M.; Fieldhouse, B.; Sigouin, L.; Landriault, M.; Smith, P.; Noonan, J.; Thouin, G., Characteristics of Spilled Oils, Fuels, and Petroleum Products: 1. Composition and Properties of Selected Oils. In Research Triangle Park, North Carolina 27711, USA: Ecosystems Research Division, United States Environmental Protection Agency, 2003; p 286.
74. Jones, D.; West, C. E.; Scarlett, A. G.; Frank, R. A.; Rowland, S. J., Isolation and estimation of the 'aromatic' naphthenic acid content of an oil sands process-affected water extract. *Journal of Chromatography A* **2012,** 1247, (1873-3778 (Electronic)), 171– 175.
75. Seifert, W. K.; Teeter, R. M., Identification of polycyclic aromatic and heterocyclic crude oil carboxylic acids. *Analytical Chemistry* **1970,** 42, (7), 750-758.
76. Bataineh, M.; Scott, A. C.; Fedorak, P. M.; Martin, J. W., Capillary HPLC/QTOF-MS for Characterizing Complex Naphthenic Acid Mixtures and Their Microbial Transformation. *Analytical Chemistry* **2006,** 78, (24), 8354-8361.
77. Martin, J. W.; Han, X.; Peru, K. M.; Headley, J. V., Comparison of high- and low-resolution electrospray ionization mass spectrometry for the analysis of naphthenic acid mixtures in oil sands process water. *Rapid Communications in Mass Spectrometry* **2008,** 22, (0951-4198 (Print)), 1919-1924.
78. Wei, D.; Orlandi, E.; Barriet, M.; Simon, S.; Sjöblom, J., Aggregation of tetrameric acid in xylene and its interaction with asphaltenes by isothermal titration calorimetry. *Journal of Thermal Analysis and Calorimetry* **2015,** 122, (1), 463-471.
79. Pradilla, D.; Simon, S.; Sjöblom, J., Mixed interfaces of asphaltenes and model demulsifiers part I: Adsorption and desorption of single components. *Colloids and Surfaces A: Physicochemical and Engineering Aspects* **2015,** 466, (0), 45-56.
80. Nenningsland, A. L.; Simon, S.; Sjöblom, J., Influence of Interfacial Rheological Properties on Stability of Asphaltene-Stabilized Emulsions. *Journal of Dispersion Science and Technology* **2014,** 35, (2), 231-243.
81. Andreas L. Nenningsland, B. G., Sebastien Simon, and Johan Sjöblom, Comparative Study of Stabilizing Agents for Water-in-Oil Emulsions. *Energy & Fuels* **2011,** 25 (12), 5746–5754.

82. Dewick, P. M., Acids and bases. In *Essentials of Organic Chemistry: For Students of Pharmacy, Medicinal Chemistry and Biological Chemistry*, Dewick, P. M., Ed. WILEY: West Sussex, England, 2006; p 130.
83. Passade-Boupat, N.; Rondon Gonzalez, M.; Hurtevent, C.; Brocart, B.; Palermo, T., Risk Assessment of Calcium Naphtenates and Separation Mechanisms of Acidic Crude Oil. In *SPE International Conference and Exhibition on Oilfield Scale*, Society of Petroleum Engineers: Aberdeen, UK, 30-31 May, SPE 155229, 2012.
84. Reinsel, M. A.; Borkowski, J. J.; Sears, J. T., Partition Coefficients for Acetic, Propionic, and Butyric Acids in a Crude Oil/Water System. *Journal of Chemical & Engineering Data* **1994,** 39, (3), 513-516.
85. Dudek, M.; Kancir, E.; Øye, G., Influence of the Crude Oil and Water Compositions on the Quality of Synthetic Produced Water. *Energy & Fuels* **2017,** 31, (4), 3708-3716.
86. Christiansen, I. Isolation and Characterization of Oil-Soluble Calcium Naphthenates in North Sea Heavy Crude Oil. M.Sc. Thesis, NTNU, Trondheim, Norway, 2014.